ARTICLE IN PRESS
PALAEO-06049; No of Pages 17
Palaeogeography, Palaeoclimatology, Palaeoecology xxx (2012) xxx–xxx
Contents lists available at SciVerse ScienceDirect
Palaeogeography, Palaeoclimatology, Palaeoecology
journal homepage: www.elsevier.com/locate/palaeo

Late Quaternary linkage of sedimentary records to three astronomical rhythms and the Asian monsoon, inferred from a coastal borehole in the south Bohai Sea, China

Liang Yi [a,b,c,*], Hong-Jun Yu [a], Joseph D. Ortiz [c], Xing-Yong Xu [a], Shen-Liang Chen [d], Jun-Yi Ge [e], Qing-Zhen Hao [e], Jing Yao [a], Xue-Fa Shi [a], Shu-Zhen Peng [f]

[a] *Key Laboratory of Marine Sedimentology and Environmental Geology, First Institute of Oceanography, State Oceanic Administration, Qingdao 266061, China*
[b] *State Key Laboratory of Loess and Quaternary Geology, Institute of Earth Environment, Chinese Academy of Sciences, Xi'an 710075, China*
[c] *Department of Geology, Kent State University, Kent 44242, USA*
[d] *State Key Laboratory of Estuarine and Coastal Research, East China Normal University, Shanghai 200062, China*
[e] *Key Laboratory of Cenozoic Geology and Environment, Institute of Geology and Geophysics, Chinese Academy of Sciences, Beijing 100029, China*
[f] *Key Laboratory of Tourism and Resources Environment in Universities of Shandong, Taishan University, Tai'an 271021, China*

ARTICLE INFO

Article history:
Received 12 March 2011
Received in revised form 10 February 2012
Accepted 14 February 2012
Available online xxxx

Keywords:
Late Quaternary
Marine records
Orbital forcing
Asian monsoon
Bohai Sea
Nonlinear climatic response

ABSTRACT

The Bohai Sea was formed by subsidence during the Cenozoic. Some 2000–3000 m of fluvial, lacustrine and marine sediments has been deposited in this basin. Previous studies focused mainly on the transgression history, with little examination of orbital variation in relation to other areas within the Asian monsoon domain. Here, we present the late Quaternary results of a new borehole in the south Bohai Sea. Optically stimulated luminescence and radiocarbon dating, which provide concordant age estimates, were employed to generate an initial chronology for the borehole. After refining the chronology through astronomical tuning, the results showed that: (1) the grain size variation represents Asian monsoon intensity which was dominated by both solar insolation (major) and global ice volume (minor) forcing; (2) the magnetic susceptibility indicates river incision processes which were sensitive to orbital tilt with influence from solar insolation; (3) the vegetation coverage responded to global ice volume coupled obliquity changes; and that (4) neither external nor internal factors could dominate the paleoenvironmental evolution on orbital timescales in an independent way, and they are both integrated in a complex pattern. We conclude that three different astronomical rhythms have affected coastal evolution, and that the sedimentary records in the south Bohai Sea, China, result from the nonlinear interaction and the complex response to driving processes.

1. Introduction

The Asian Monsoon plays an important role in transporting large quantities of heat and moisture to the most populated regions of the world. These heat and moisture values, having profound effects on social processes especially in the agriculture era (e.g. Cook et al., 2010; Yancheva et al., 2007; Zhang et al., 2008a), have attracted great attention in palaeoenvironmental studies over the past few decades (e.g. Wang, 2006). Due to the limitation of relevant modern records, the studies on monsoon-modulated heat and moisture variation have been conducted using proxy indicators such as Chinese loess (e.g. An et al., 1990, 2001; Ding et al., 1995; Guo et al., 2002; Kukla, 1987; Liu, 1985; Liu and Ding, 1993; Sun et al., 2006, 2012), cave records (e.g. Cheng et al., 2009; Wang et al., 2001, 2005, 2008; Zhang et al., 2008a), tree rings (e.g. Cook et al., 2010; Shao et al., 2010; Treydte et al., 2006), lacustrine sediments (e.g. An et al., 2011; Xiao et al., 2009; Yancheva et al., 2007) and marine sediments (e.g. Ao et al., 2011; Clemens and Prell, 2003; Tian et al., 2008; Wang et al., 1999; Wehausen and Brumsack, 2002), to extend our understanding of the evolution of the monsoon system.

Although there have been numerous studies conducted on Asian monsoon evolution during the past thirty years, its mechanism is still in keenly debated. Depending upon proxy records studied, there are two scenarios most commonly invoked to describe the mechanism of Asian monsoon evolution: internal *vs.* external forcing models.

The internal forcing of Asian monsoon evolution stipulates that the global ice volume plays a controlling influence on the Asian monsoon by modulating the thermodynamic difference between the Asian continent and the Pacific Ocean (An et al., 1990). During an interglacial stage, the enlarged pressure gradient between continent and ocean enables the monsoon to carry greater fluxes of heat and moisture from ocean to continent, while during a glacial stage, the weakened monsoon causes smaller fluxes of heat and moisture from ocean to continent. Variations of global ice volume can influence

* Corresponding author at: Key Laboratory of Marine Sedimentology and Environmental Geology, First Institute of Oceanography, State Oceanic Administration, Qingdao 266061, China.
E-mail addresses: yi.liang82@gmail.com, crane_yi@yahoo.com.cn (L. Yi).

0031-0182/$ – see front matter © 2012 Elsevier B.V. All rights reserved.
doi:10.1016/j.palaeo.2012.02.020

the Asian monsoon in three ways: (1) Global ice volume affects global sea levels and varies relative surface areas between continent and ocean. The increased continental surface area during a glacial stage can increase the loss of heat and moisture being transported from ocean to continent (Wang, 1999). (2) Global ice volume can affect global temperature. Decreased sea surface temperature can reduce evaporation and thus decrease moisture (Guo et al., 2002, 2004). (3) The extended Arctic ice sheet may strengthen the Siberian-Mongolian Highs during a glacial stage, and increase the Asian winter monsoon and reduce the heat and moisture carried from ocean (Ding et al., 1994). Through these possible responses, the Asian monsoon documented in various sediments is considered to be dominated by 100-ka cycles and many inland-related records support this inference (e.g. An et al., 1990, 2001, 2011; Ding et al., 1995; Kukla, 1987; Liu, 1985; Liu and Ding, 1993; Liu et al., 1999; Sun et al., 2006, 2012; Wang, 1999; Wang et al., 1999; Wehausen and Brumsack, 2002).

The external model of Asian monsoon evolution stresses the importance of variation in solar insolation as the direct driving factor controlling climatic changes. According to this model, the monsoon is interpreted as an intertropical convergence zone (ITCZ) substantially away from the equator (more than 10°) and the existence of ITCZ does not have to rely on land–sea contrast which only provides a favorable longitudinal location for the ITCZ (Chao and Chen, 2001). The ITCZ with maximal solar heating is one of the most intensive suppliers of vapor and energy from ocean to atmosphere (Pierrehumbert, 2000). The ascending flow from the ITCZ makes up the upward branch of monsoon circulation, which brings about aridity to the region of its descending flow and maximal precipitation to the region of its ascending flow (Webster et al., 1998). The ascending solar insolation increases the sea surface temperature which causes the northward movement of ITCZ and strengthened Asian monsoon, while the descending solar insolation causes the southward movement of the ITCZ that, coupled with the decreased sea surface temperature, weakens the Asian monsoon. Because in this scenario the Asian monsoon is directly controlled by solar insolation, its variability is assumed to be predominantly expressed as precessional cycles, i.e. 19–23 ka, and this inference has been supported by many low-latitude studies (e.g. Wang et al., 2001, 2005, 2008; Cheng et al., 2009; Ao et al., 2011).

However, in reality, Asian monsoon is likely controlled both by internal and external factors (Wang, 2009). The record from the Indian Ocean showed that the monsoon was sensitive to the latent heat export from the southern subtropical Indian Ocean (Clemens et al., 1991) and was controlled mainly by obliquity rather than precession (Clemens and Prell, 2003). Through analyzing the phase difference between the south China cave $\delta^{18}O$ (Cheng et al., 2009; Wang et al., 2001, 2008) and maximum northern hemisphere summer insolation, Clemens et al. (2010) argued that the "pure" Asian monsoon proxy, i.e. the south China cave $\delta^{18}O$, essentially combined the influence of summer monsoon (major) and winter temperature (minor) forcing. Thus, the Asian monsoon fundamentally associates the complex behavior of atmosphere and ocean, and it is critical to obtain more evidences from various environments to help understanding the complexity of monsoonal climate.

The Bohai Sea is a semi-enclosed interior continental shelf sea of China, which is connected to the northern Yellow Sea by the narrow Bohai Strait with an average water depth of 18 m (IOCAS, 1985). During the past thirty years, the sediments of Bohai Sea have been involved in environmental and geological research, and these studies mainly focused on sea level changes and its environmental impacts (Liu, 2009). The results on orbital timescales with regard to the Late Quaternary are contained in IOCAS (1985), Liu (2009) and references therein: (1) sea level history has been recorded in alternations between terrestrial and marine sediments and controlled by glaciations and deglaciations; (2) transgressions are evident at the beginning of interglacial stages including the Holocene, marine isotope stage 3 (MIS3) and MIS5; and (3) regressions are recorded at the beginning of glacial stages, MIS2 and MIS4.

Because the Bohai Sea is close both to the Asian mainland and the Pacific Ocean and is influenced both by the Siberian–Mongolian Highs and the ITCZ (Fig. 1), it is possible that the deposits in Bohai Sea record the interaction between various driving factors. However, in previous studies little attention has been paid in this potential interaction. Therefore, to generate more evidence correlating palaeoenvironmental evolution and to detect the potential interaction between various driving factors on orbital timescales, we chose a new borehole drilled in the south Bohai Sea in 2007 for the present study of the late Quaternary. Optically stimulated luminescence and radiocarbon dating were employed to produce the borehole's chronology. After refined the chronology through astronomical tuning, we attempted to reveal the potential relationship between three astronomical rhythms (eccentricity, obliquity and precession) and the Asian monsoon and provide evidence for the complex behavior of atmosphere and ocean.

2. Study area and materials

2.1. Geological settings

The south Bohai Sea (Laizhou Bay, Fig. 1) is located between the branches of the Yi-Shu Rift (Gao et al., 1980; Zhang et al., 2003). The period from the Neogene to the present has been marked by tectonic quiescence and stable sedimentation (Wu et al., 2006; Yu et al., 2008). Sedimentary alternations were mainly between deltaic, estuarine and tidal plain systems (Xue and Ding, 2008). During regressions, the exposed area of the south Bohai Sea would have been replaced in part by diluvial fan (Chen et al., 1991), loess/sandy dune (Chen et al., 1991; Yu et al., 1999; Zhao, 1991, 1995) or alluvial fan (Meng et al., 1999).

The sediments in the south Bohai Sea were deposited by several local rivers including the Xiaoqinghe River, Mihe River and Weihe River (Xue and Ding, 2008). All of these rivers, only 100–300 km long originate in the Luzhong Mountain Range where the elevation is 800–1600 m. The average slope for the whole catchments is 0.05–0.11‰.

2.2. Borehole Lz908

Borehole Lz908 is located on the south coast of the Bohai Sea, China (37°09′N, 118°58′E; elevation 6 m; Fig. 1). The drilling position was covered by seawater until the middle of the twentieth century. The length of core is 101.3 m and the recovery rate is 75%. The upper 54 m contained fluvial and coastal sediments and were chosen here for study. According to the fossil foraminifera assemblages of Lz908 core, Yao et al. (2010) identified three transgression layers and the depth was modified in this paper: 2.0–11.3 m (transgression 1, T-1), 14–28.2 m (transgression 2, T-2) and 36.4–50.3 m (transgression 3, T-3). The sedimentary descriptions are as follows (Fig. 2):

2.0–4.9 m, yellowish grey fine sand, high water content and mollusk debris. (Tidal flat-Delta). *9–10.2 m*, dust-color fine sand, high water content and mollusk debris. (Intertide-Delta). *10.2–10.8 m*, dark-grey and black organic-rich clay, mollusk and vegetation debris. (Lagoon). *10.8–15.2 m*, yellow–grey coarse silt, red patches and dark-grey organic-rich veins. (Lagoon-Alluvial fan). *15.2–19.2 m*, mahogany and yellowish grey clay–silt, high water content and mollusk debris. (Delta-Alluvial fan). *19.2–22.5 m*, yellowish grey coarse silt, high water content, mollusk debris and red patches. (Intertide-Delta). *22.5–26.2 m*, dark red and yellowish grey clay, and red patches. (Intertide-Delta). *26.2–27.4 m*, yellowish grey coarse silt, high water content, and mollusk debris and red patches. (Intertide-Delta). *27.4–31.3 m*, dust-color clay, mollusk debris and very hard. (Intertide-Delta). *31.3–34.2 m*, yellowish grey clay–silt, vegetation and mollusk debris, and red patches. (Lagoon-Delta). *34.2–36.2 m*, dust-color clay, carbonate nodules and mollusk debris, and very hard.

Please cite this article as: Yi, L., et al., Late Quaternary linkage of sedimentary records to three astronomical rhythms and the Asian monsoon, inferred from a coastal boreho..., Palaeogeogr. Palaeoclimatol. Palaeoecol. (2012), doi:10.1016/j.palaeo.2012.02.020

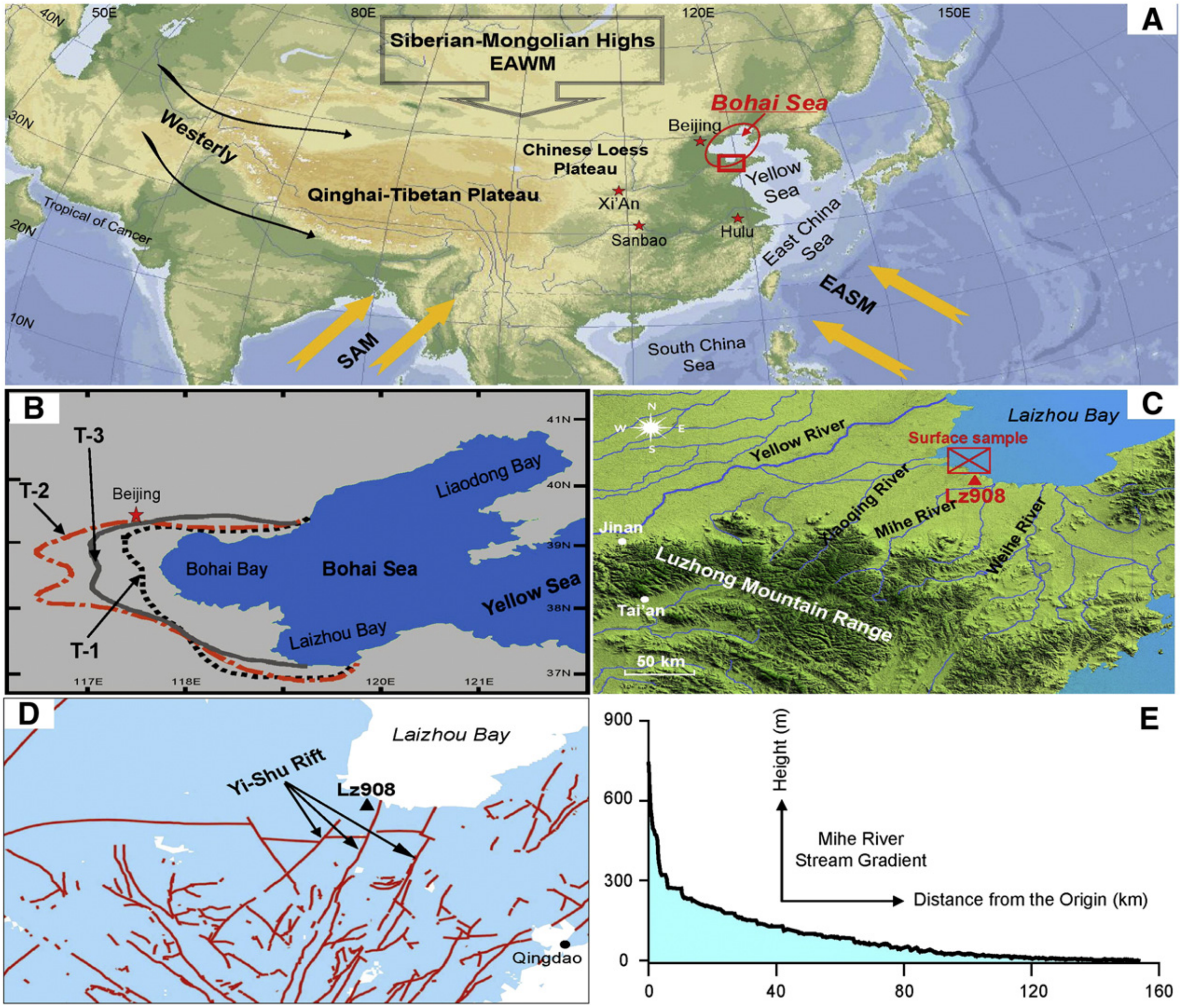

Fig. 1. (A) Location, climatic systems, and sites mentioned in the text. The East Asian Summer Monsoon (EASM), East Asian Winter Monsoon (EAWM) and the Westerly system predominantly control the regional climate. SAM is an abbreviation of South Asian monsoon. (B) Shoreline changes of each transgression relate to the late Pleistocene. Lines represent the margins of transgression-1 (T-1), transgression-2 (T-2) and transgression (T-3), respectively. It is modified from Zhao (1986) and Wang et al. (1986). (C) Geographical settings, drainage system, the position of borehole Lz908 (▲) and the area where surface sediments were taken. (D) Distribution of faults within the study area. (E) Stream gradient of the Mihe River from the Luzhong Mountain Range to the south Bohai Sea.

(Lagoon-Delta). *36.2–38.9 m*, mottled fine silt, and dark-grey organic-rich veins. (Intertide-Delta). *38.9–41.9 m*, dust-color coarse silt, olive-grey carbonate veins and nodules, and very hard. (Lagoon-Delta). *41.9–44.6 m*, mahogany fine silt, olive-grey veins, and very hard. (Lagoon-Delta). *44.6–48.2 m*, yellowish grey coarse silt, high water content, and mollusk debris. (Intertide-Delta). *48.2–51.4 m*, grey fine silt, pores and mollusk debris. (Intertide-Delta). *51.4–54.3 m*, grey and yellow-grey coarse silt, carbonate nodules and very hard. (Delta-Lake).

2.3. Surface sediments

Thirty-six marine surface sediment samples were collected around the estuarine area outside the Xiaoqinghe river mouth (Fig. 1) during Jan 23rd–29th, 2007, by the Institute of Oceanology, Chinese Academy of Sciences. During the field investigation, the weather was calm with little wave activity (Chen et al., 2009; Du et al., 2008).

3. Methodology

3.1. Experiments

Three proxy indices were employed, grain size, magnetic susceptibility and tree-pollen abundance, to infer palaeoenviromental changes (Fig. 2). The interval between grain size samples is about 2–5 cm, and a total of 1771 samples were measured. The grain size samples were pretreated with 10–20 ml of 30% H_2O_2 to remove organic matter, washed with 10% HCl to remove carbonates, rinsed with deionized water, and then placed in an ultrasonic vibrator for several minutes to facilitate dispersion. One hundred grain size classes between 0.3 and 300 μm were exported using a Malven Mastersizer 2000 analyzer.

Magnetic susceptibility (MS) was measured at 10–20 cm intervals using a Bartington Instruments MS2 magnetic susceptibility meter, and a total of 373-data points were produced.

Pollen was extracted from coastal sediments using the integrative method of sieving and heavy liquid separation (Li and Du, 1999). A total of ninety-nine samples were investigated at ~50 cm intervals in the Center of Hydrogeology and Environmental Geology, China Geology Survey. The pollen count per 100-gram bulk sample ranges from 2 to 279, with an average value of 150.

To detect the potential relationship between the three proxies, scatter plots were employed showing that there was no obvious correlation between the three proxies (Fig. 3). However, because the median grain size was related to the sedimentary changes (CDIG, 1978), it is implied that the magnetic susceptibility and the tree-pollen abundance are independent of the sedimentary variation

Please cite this article as: Yi, L., et al., Late Quaternary linkage of sedimentary records to three astronomical rhythms and the Asian monsoon, inferred from a coastal boreho..., Palaeogeogr. Palaeoclimatol. Palaeoecol. (2012), doi:10.1016/j.palaeo.2012.02.020

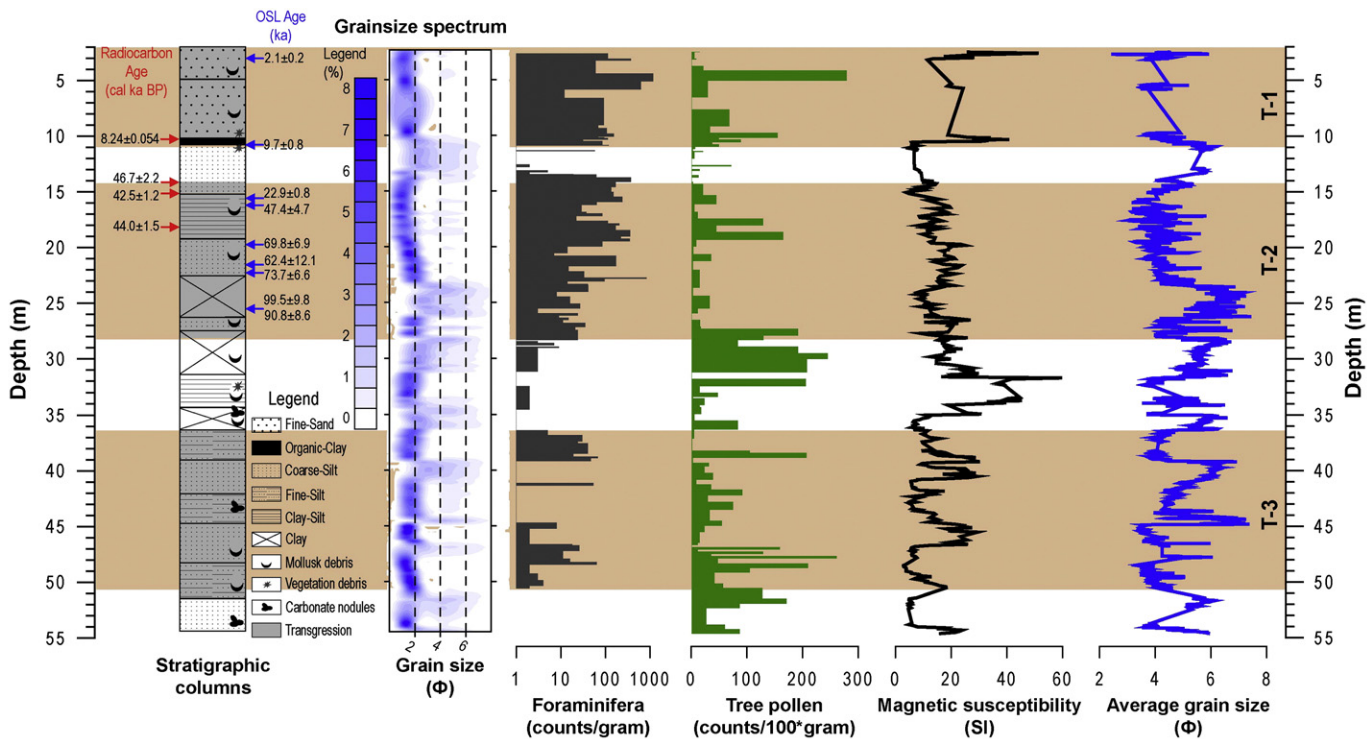

Fig. 2. Stratigraphic columns, grain size spectrum, radiocarbon dates and OSL ages, foraminifera counts and the three proxies of the borehole Lz908. The depth of three transgressions is marked as shadows. The foraminifera data is from Yao et al. (2010).

indicating that these two series could be used as palaeoenvironmental indicators.

3.2. Grain size indicator

Sediment grain size is a powerful proxy applied in various paleoenvironmental studies. For instance, the grain size of loess–paleosol sequences is regarded as a good index of East Asian Winter Monsoon (EAWM) intensity: coarser grain size corresponds to strengthened EAWM, and finer grain size corresponds to weakened EAWM (e.g., An et al., 1990, 1991; Ding et al., 1994; Guo et al., 1998; Liu and Ding, 1998; Porter and An, 1995; Sun et al., 2006, 2012). On the other hand, Sun (2004) stated that the grain size distribution of the late Cenozoic aeolian deposition could be divided into two groups-fine and coarse parts-which might relate the high-altitude westerly stream and the low-altitude winds of monsoonal circulation, respectively. For lacustrine sediments, the coarser grain size might indicate moister periods: high discharge brings coarse sediments into lake, the outflow discharge removes fine-grained sediments, and the net effect of these two processes produces coarse sediments (Campbell, 1998). In contrast, White (2002) argued that increased grain size is caused by a warmer and drier climate in which lake levels decrease and the inflowing drainage systems eroded to a lower local base level. For coastal sediments, the coarse grains could indicate the high-energy environment in offshore areas controlled by coastal or tidal processes (e.g. Zhang et al., 2008b), or high precipitation in onshore areas dominated by fluvial input (e.g., Boulay et al., 2007; Liu et al., 2005). Hence, because of the complicated sedimentary dynamics, it is necessary to assess possible changes of various processes involved in deposition. To achieve this, we employed varimax-rotated Principle Component Analysis (V-PCA) using the correlation matrix of grain size spectra for grain sizes ranging from 0.3 to 300 μm as the input matrix. This method assumes that each sedimentary process is related with a specific grain size spectral shape, and thus allows us to separate out orthogonal modes (independent grain size spectral components/shapes) indicating potential changes of input functions (Darby et al., 2009; Weltje, 1997).

As an initial step, to test the underlying assumption, we performed separate V-PCA analysis on the transgressive, regressive and surface data sets, and then combined the surface and core data to analyze their components in common. The loess grain size collected from the Xifeng Profile on the Chinese Loess Plateau (Hao et al., 2008) was also compared for reference. This allowed us to test the null hypothesis that different processes control the sedimentation in these data sets (Darby et al., 2009). The results show that all of the surface, transgressive and regressive sediments have the same data structure as seen in nearly identical component loading models, but the loess samples was completely different (Fig. 4). This relation was also observed from the comparison among various samples with the same data structure (Fig. 5). Thus, it is inferred that the factors dominating grain size variation during transgressive–regressive alternations did not change obviously, but the relative importance (percentage) of each component varied with time.

The sediments in the south Bohai Sea were deposited from several local rivers, all of which originate from the Luzhong Mountain Range. Because the sedimentary facies altered between delta, tidal flat and inter-tide systems during a transgression and between delta, alluvial and lagoon environments during a regression, the constant factor controlling the grain size variation could only be the fluvial processes and the four components extracted from V-PCA procedures may correspond to the differences between these local rivers in water discharge, sediment loads or topography. Additionally, there is a slight difference in the clay component (finer than 4 μm) in Fig. 5C, indicating that other processes only have a small influence on component F4 of transgressive sediments. Considering the environmental differences between transgression and regression, these recessive factors might be correlated to coastal or source-area settings.

Please cite this article as: Yi, L., et al., Late Quaternary linkage of sedimentary records to three astronomical rhythms and the Asian monsoon, inferred from a coastal boreho..., Palaeogeogr. Palaeoclimatol. Palaeoecol. (2012), doi:10.1016/j.palaeo.2012.02.020

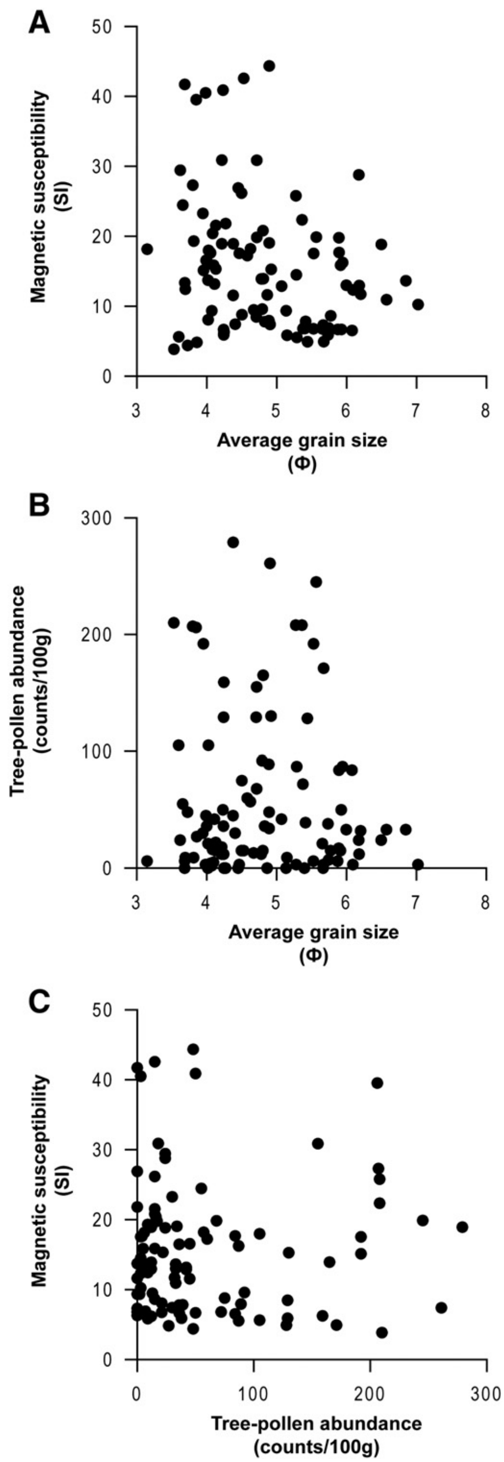

Fig. 3. Correlation between median grain size and magnetic susceptibility (A), median grain size and tree-pollen abundance (B), magnetic susceptibility and tree-pollen abundance (C).

4. Absolute dating and initial timescale

4.1. Transgressions around the Bohai Sea

In the west Bohai Sea, Zhao et al. (1978) initially reported three transgressions based on 71 coastal cores and their depth ranges were 5.0–16.8 m (T-1), 27.5–43.9 m (T-2) and 56.2–79.9 m (T-3), respectively. Most subsequent works around the marginal seas of China (South China Sea, East China Sea, Yellow Sea and Bohai Sea) stated comparable results in sedimentary characteristics (see the reviews of Wang and Tian, 1999; Liu, 2009; Fig. 6). Wang and Tian (1999) analyzed the neo-tectonic setting of the late Quaternary transgression in the eastern coastal plain of China and reviewed the T-3 base in the west of the Bohai Sea. In the south Bohai Sea, Han et al. (1994) reported the depths of T-1, T-2 and T-3 as 0–18.5 m with a thickness of 5–10 m, 12–50 m with a thickness of 10–25 m, and 35–76 m with a thickness of 10–15 m, respectively. Zhang et al. (1996) reviewed 17 cores and concluded the depths of T-1, T-2 and T-3 are 2–27 m, 15–32 m and 30–48 m, respectively. Based upon the fossil foraminifera assemblages of Lz908 core, Yao et al. (2010) correlated the transgressive/regressive events with the Shouguang E core (Zhao, 1995).

The age model for these transgressions could be summarized as follows (Zhao et al., 1978; IOCAS, 1985; Liu, 2009, also see Fig. 6): (1) constrained by radiocarbon dating, T-1 developed in the Holocene; (2) constrained by the radiocarbon, TL/OSL and geomagnetic excursion (Mungo Event, 35–40 ka, Barbetti and McElhinny, 1976), T-2 developed in MIS3; (3) constrained by the geomagnetic excursion (Black Event, 110–120 ka, Smith and Foster, 1969), T-3 developed in MIS5; and (4) regressions occurred at the beginning of glacial stages, i.e. MIS2 and MIS4. Based upon regional comparisons, this time framework was employed in the marginal seas of China (Liu, 2009). Similarly, based on the events correlated with the Shouguang E core (Zhao, 1995), Yao et al. (2010) suggested the ages of T-1, T-2 and T-3 in the Lz908 core were the Holocene, MIS3 and MIS5, respectively.

4.2. Absolute dating of Lz908 core

4.2.1. Radiocarbon dating

Four foraminifer samples from Lz908 were taken for radiocarbon dating. All radiocarbon measurements were conducted at Woods Hole Oceanographic Institution in the USA using the Accelerator Mass Spectrometry method (AMS). The conventional ages were converted to calendar ages using the Calib6.0 radiocarbon calibration program (Stuiver and Reimer, 1993) with the Bohai Sea calibration dataset (Wang and Fan, 2005; Wang et al., 2004). The dating results are summarized in Table 1.

4.2.2. OSL dating

For the optically stimulated luminescence (OSL) dating, we chose pure quartz of the fine fraction (4–11 μm) and followed the sensitivity-corrected multiple aliquot regenerative-dose protocol developed by Lu et al. (2007) to determine the equivalent dose. All measurements were performed using a Daybreak 2200 automated OSL reader in Qingdao Institute of Marine Geology, Chinese Geological Survey. Following Aitken (1998) and Prescott and Hutton (1994), we then measured neutron activation and cosmic ray contribution in the dose rate determination, while taking into account influences from water content and grain size. The dating results are summarized in Table 2.

4.2.3. Dating results

For T-1, there is one radiocarbon date, i.e. 8.24 ± 0.054 cal ka BP, and two OSL ages, i.e. 2.1 ± 0.2 ka and 9.7 ± 0.8 ka (Figs. 2 and 7). These three ages constrain T-1 to the Holocene, which is consistent with previous studies (Wang and Fan, 2005; Wang et al., 2004). Additionally, the age-depth relation also demonstrates that the ages within errors are consistent between radiocarbon and OSL methods.

For the pre-Holocene samples, there are three radiocarbon dates, i.e. 46.7 ± 2.2, 42.5 ± 1.2 and 44.0 ± 1.5 cal ka BP, and seven OSL ages from 22.9 ± 2.0 ka to 99.5 ± 9.8 ka. These radiocarbon dates and OSL ages are stratigraphically consistent with depth ($r = 0.97$, $p < 0.01$) constraining T-2 to MIS3-5 (Fig. 7). This result is somewhat similar to those of Yim et al. (1990) and Chen et al. (2008) but different

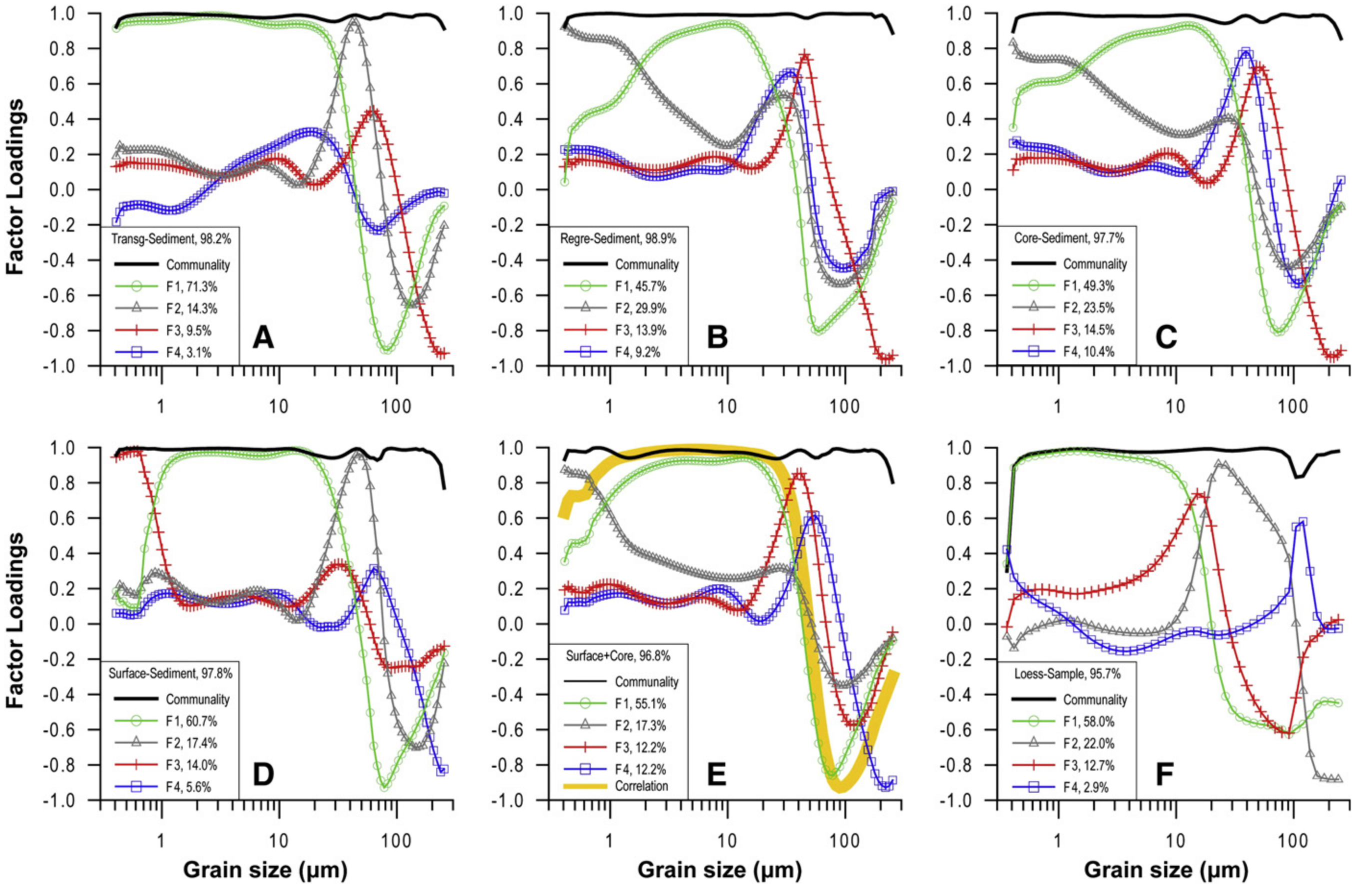

Fig. 4. V-PCA results from different types of samples. A (Transg-Sediment), transgressive samples; B (Regre-Sediment), regressive samples; C (Core-sediment), the whole samples from Lz908 core; D (Surface-Sediment), surface samples (Chen et al., 2009; Du et al., 2008); E (Surface + core), combined surface samples and Lz908 core samples; and F (Loess-Sample), loess sediments from Xifeng Profile (Hao et al., 2008). F1, F2, F3 and F4 represent the components of V-PCA procedures and their variances are displayed.

from other studies (e.g. IOCAS, 1985; Lin et al., 2005; Wang and Tian, 1999; Zhang et al., 2008b; Zhao, 1995; Zhao et al., 1978).

4.2.4. MIS-3 Problem related to the transgression ages

Although the transgressions around the marginal seas of China are comparable (Fig. 6, see the reviews of Wang and Tian, 1999; Liu, 2009), there are some debates about their ages with most attentions paid to T-2. Three questions related to T-2 have not been answered yet (see the review of Liu, 2009): (1) T-2 was buried at a depth of 15–40 m, while ^{14}C ages range from 38 to 24 ka for the top of T-2, and from 35 to 23 ka for the bottom. The age intervals overlap, and which one should be trusted (Liu, 2009)? (2) Compared with the borehole QC2 located in the south Yellow Sea and dated to 28.5 ka by ^{14}C at the beginning of T-2 (Fig. 6, Yang and Lin, 1991), why and how did T-2 occur in the Bohai Sea (35–40 ka) earlier than in the Yellow Sea (Liu, 2009)? (3) In the context of global sea level 60–80 m lower in MIS 3 than the present (Chappell et al., 1996), why and how did this transgression occur and have a greater influence than T-3 (Fig. 1B)?

One possible explanation could be related to the chronologies, which were estimated mainly by counting transgression strata and measuring geomagnetic excursions (Liu, 2009). Based upon the comparison between U-series and radiocarbon dates of borehole sediments, Yim et al. (1990) stated that T-2 deposited in Hong Kong should have formed in MIS 5 but not in MIS 3. Chen et al. (2008) also argued that T-2 was constrained to MIS 5 based upon OSL dating. According to radiocarbon and OSL dating results in the Lz908 core sediments, T-2 was supposed to occur at the beginning of MIS 5 supporting the conclusions of Yim et al. (1990) and Chen et al. (2008).

4.3. Hiatuses and preliminary timescale

4.3.1. Sedimentary hiatuses

Between alternations of transgression and regression, there could be some hiatuses due to paleoenvironmental changes. Li et al. (2004) suggested that there were five hiatuses in the three transgressions based upon the sedimentation and age characteristics of six boreholes in the west Bohai Sea (Table 3). However, it seems that the hiatuses in the west Bohai Sea lasted less than 10 ka indicating no major hiatus during the three alternations between transgression and regression. In contrast, based upon OSL dating, Chen et al. (2008) argued that the sedimentary process in Tianjin area was predominantly eroded and that the transgressive sediments were deposited in a very short period.

However, the south Bohai Sea is located between the branches of the Yi-Shu Rift (Gao et al., 1980; Zhang et al., 2003) which are components of the Tan-Lu Rift System. Continuous subsidence (Wu et al., 2006; Yu et al., 2008) provides an appropriate condition for preservation of sedimentary strata. The sediments transported from the Luzhong Mountain Range is carried by local rivers with steep stream gradients (8–15 m/km), which drops suddenly where the rivers reach the coastal plains, decreasing their gradient to 0.1–0.5 m/km as they progress towards the south Bohai Sea. The gradient pattern of the drainage system indicates that these local rivers have a large and constant capacity to carry various grains from mountains to coastal plains. Moreover, because of the short distance between sediment source and deposition, when a regression occurred, the study area have been replace by diluvial fan (Chen et al., 1991), loess/sandy dunes (Chen et al., 1991; Yu et al., 1999; Zhao, 1991; 1995) or alluvial fan (Meng et al., 1999). Thus, because of these geomorphologic and

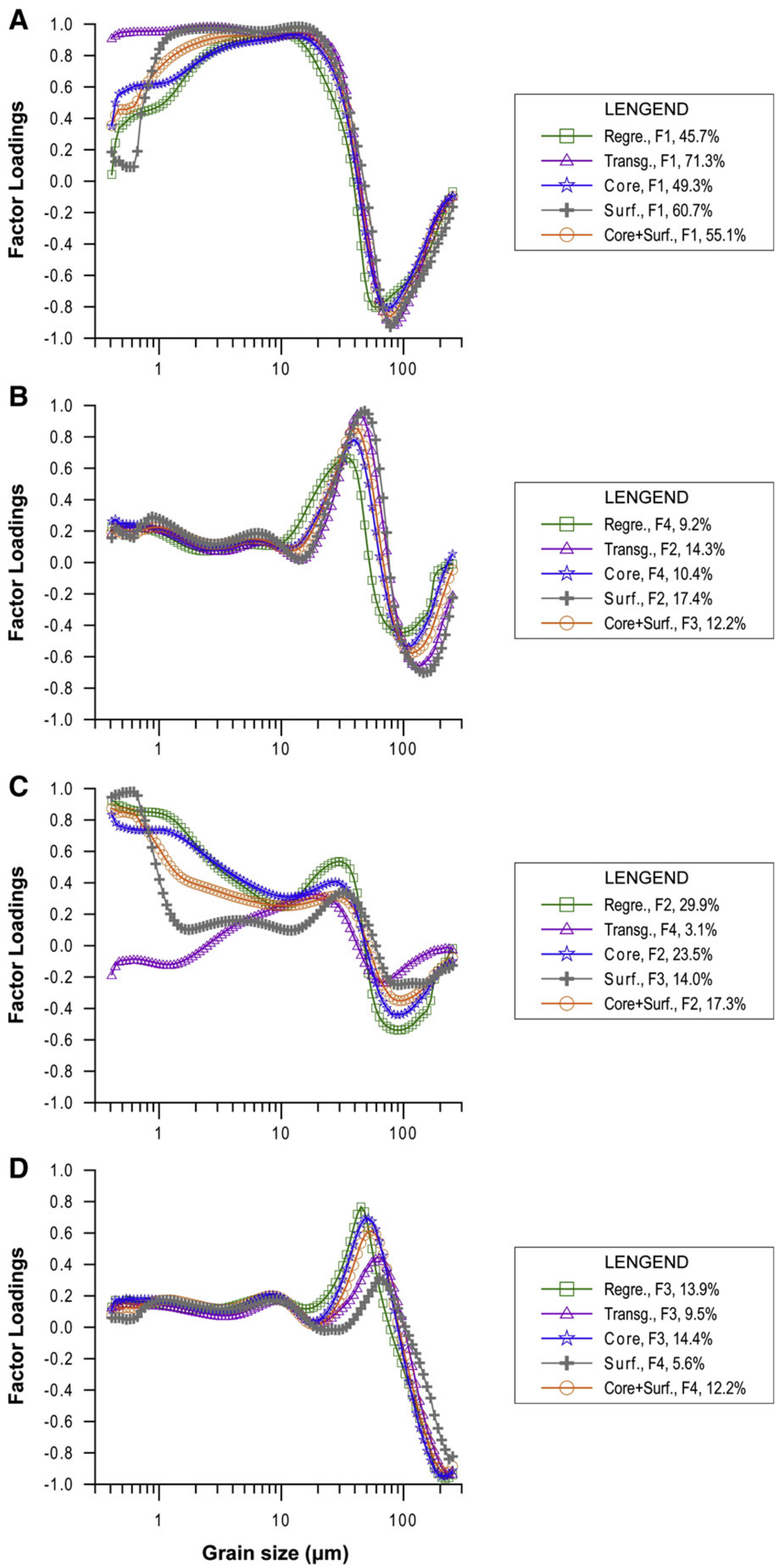

Fig. 5. V-PCA result comparisons within the same data structures. The abbreviations are same as in Fig. 4.

Please cite this article as: Yi, L., et al., Late Quaternary linkage of sedimentary records to three astronomical rhythms and the Asian monsoon, inferred from a coastal boreho..., Palaeogeogr. Palaeoclimatol. Palaeoecol. (2012), doi:10.1016/j.palaeo.2012.02.020

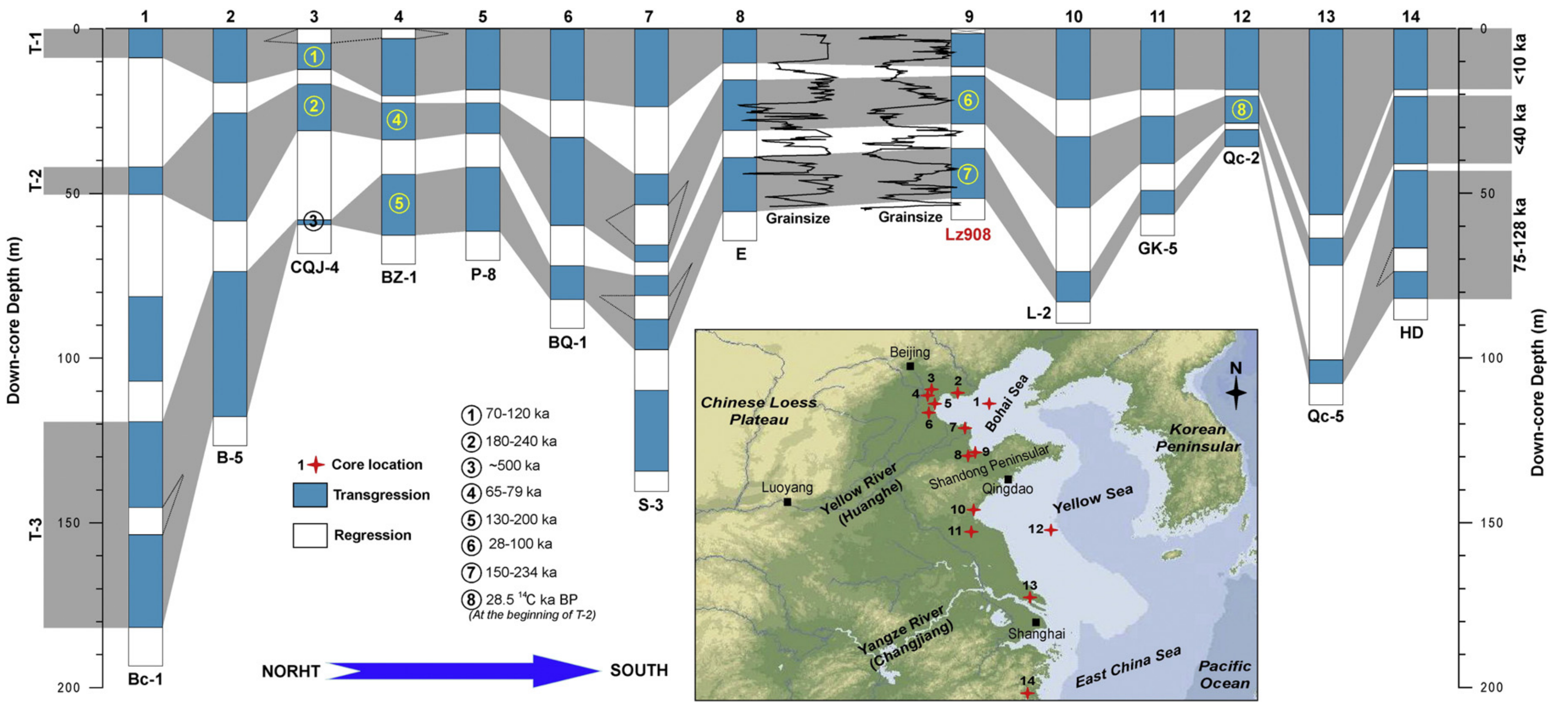

Fig. 6. Regional comparison of the three transgressions around the Bohai Sea and the Yellow Sea. 1, Bc-1 (IOCAS, 1985); 3, CQJ-4 (Shi et al., 2009); 4, BZ-1 (Chen et al., 2008); 5, P-8 (Gao et al., 1986); 6, BQ-1 (Yan et al., 2006); 7, S-3 (Zhuang et al., 1999); 8, E (Zhao, 1995); 9, Lz908 (this study); 12, Qc-2 (Yang and Lin, 1991); 2 (B-5), 10 (L-2), 11 (GK-5), 13 (Qc-5) and 14 (HD) are modified from Wang and Tian (1999). The average grain size of E core (Zhao, 1995) and Lz908 core (this study) are also displayed for comparison. The ages of three transgressions were constrained to <10 ka, <40 ka and 75–128 ka, respectively (Wang and Tian, 1999), and five different reports are labeled ①–⑧. See details in text.

Table 1
Radiocarbon dates on materials from the borehole Lz908.

Samples ID	Lab. No.	Depth (m)	Dating type	F Modern	Date	Date*	Date interval**	d^{13}C	Δ^{14}C
					(^{14}C yr BP)	(cal ka BP)	(cal ka BP)		
LZ908-1(^{14}C),	OS-83158	10.10–10.20	Mixed Foraminifera	0.3854 ± 0.0016	7660 ± 35	8.240 ± 0.054	8.132–8.348	−7.33	−617.30
LZ908-2(^{14}C),	OS-83159	14.00–14.10	Mixed Foraminifera	0.0045 ± 0.0016	43400 ± 2900	46.7 ± 2.2	42.3–51.1	−3.35	−995.52
LZ908-3(^{14}C),	OS-83160	15.10–15.20	Mixed Foraminifera	0.0087 ± 0.0016	38200 ± 1500	42.5 ± 1.2	40.1–44.9	−3.31	−991.41
LZ908-4(^{14}C)	OS-83179	18.10–18.20	Mixed Foraminifera	0.0065 ± 0.0016	40400 ± 2000	44.0 ± 1.5	41.0–47.0	−3.42	−993.53

Note: *The conventional dates were converted to a calibrated age using the Calib6.0 radiocarbon calibration program (Stuiver and Reimer, 1993) with the Bohai Sea calibration dataset (Wang and Fan, 2005; Wang et al., 2004). **Confident intervals of radiocarbon date at 95.4% confident level.

topographic features, there was no large sedimentary hiatus evident in the south Bohai Sea (Han et al., 1994; Lin et al., 2005; Liu et al., 2009; Zhao, 1995). Moreover, the grain size spectra of Lz908 core exhibits no abrupt changes and the sediments are compositionally homogeneous downcore (Fig. 2), and the radiocarbon dates and OSL ages, within errors, are generally stratigraphically consistent with depth (Fig. 7). Thus, it seems unlikely that there are any major hiatuses in the Lz908 core.

4.3.2. Preliminary timescale and sediment accumulation rate

Considering the homogeneous sediments and the correlation between the radiocarbon and OSL dating results and their depth, we infer there were no major sedimentary hiatuses in the upper 54 m of Lz908 core and chose linear interpolation and extrapolation strategies to construct a preliminary timescale for the core (Fig. 7).

The age-depth model indicates that the late Quaternary sediments in borehole Lz908 in are 54.0 m thick, which constrains the timing of T-1, T-2 and T-3 to the Holocene, MIS3-5, and MIS7, respectively. Sedimentation could be divided into two rates (Fig. 7): (1) a very high rate of 107 cm/ka in the Holocene and (2) a moderately high rate of 17 cm/ka in the pre-Holocene. The sedimentation rate in borehole Lz908 indicates that the sampling interval of 2 cm provides an averaging temporal resolution of ~18 a in the Holocene and ~117 a in the pre-Holocene. Estimates of the thickness of the Holocene sediments around the Bohai Sea range from 9 to 15 m (Wang and Fan, 2005; Wang et al., 2004), consistent with the value of ~11 m that we estimated for Lz908 core.

5. Astronomical timescale

5.1. Grain size variation vs. Asian monsoon

5.1.1. Proxy indicator

Because the river is the unchangeable factor in paleoenvironmental evolution, to include all the variations related to fluvial changes, we combined four components developed from V-PCA procedures of surface + core samples into a new series of grain size (GS):

$$GS = 55.1 \times Factor1 + 17.3 \times Factor2 + 12.2 \times Factor3 + 12.2 \times Factor4$$

According to data structure and correlation with each grain size class (Fig. 4E), this integrated series, GS, combined the variations positively from fine grains and negatively from coarse grains.

5.1.2. Interpretation of the GS series

Sediment transport can alter grain size vertically within the seabed and horizontally across the continental shelf (Wheatcroft et al., 2007): as bed shear stresses initially increase during a re-suspension event, fine sediment is re-suspended from the surface layer of the bed, leaving the coarsest sediment as a lag or armouring layer on the bed. When flow conditions wane, coarse material in suspension will settle out first, owing to its higher settling velocity and the fact that it is carried close to the seafloor, resulting re-deposited sediments will fine upward (Leithold, 1989; Nittrouer and Sternberg, 1981; Wheatcroft et al., 2007). Hydrological experiments demonstrate that grains in the 40–90 μm size range can be suspended under a flow velocity of as low as 18.57 cm/s (Chen, 1982). Because velocities of 30–40 cm/s are common in the study area (Chen et al., 2009; Du et al., 2008), many of the sediments deposited at our location will consist of winnowed materials re-suspended from the surrounding near-shore flats (Chen et al., 2009; Du et al., 2008). Additionally, the materials of the core sediments have been transported in the form of graded and uniform suspension (Yi, 2010). Thus, it is inferred that the GS series is related to the re-suspension intensity: when the flow velocity increases, the re-suspension strengthens causing that the sediment contains less coarse grains but more fine fractions, and the GS consequently increases.

Water discharge and stream gradients are two factors influencing flow velocity. The stream gradient of rivers is 0.1–0.5 m/km towards the sea and the average slope of the near-shore flat is ~0.02% with a

Table 2
Optically stimulated luminescence dating results of the borehole Lz908.

Sample	Depth	U (ppm)	Th (ppm)	K (%)	Water content	Dr (Gy/ka)	De (Gy)	Age (ka)*	Age interval (ka)**
D15	3.0 m	1.39 ± 0.015	6.30 ± 0.02	1.536	10.5 ± 5%	2.43 ± 0.18	5.08 ± 0.17	2.1 ± 0.2	1.7–2.5
D20	10.7 m	2.91 ± 0.015	9.09 ± 0.02	1.784	13.5 ± 5%	3.12 ± 0.23	30.24 ± 1.16	9.7 ± 0.8	8.1–11.3
D28	15.4 m	1.11 ± 0.015	5.00 ± 0.02	1.872	10.8 ± 5%	2.44 ± 0.19	55.77 ± 2.48	22.9 ± 2.0	18.9–26.9
D29	16.1 m	1.08 ± 0.015	5.01 ± 0.02	1.784	13.8 ± 5%	2.26 ± 0.17	106.98 ± 6.56	47.4 ± 4.7	38.0–56.8
D32	19.7 m	1.32 ± 0.015	7.18 ± 0.02	1.736	10.9 ± 5%	2.55 ± 0.19	178.15 ± 11.32	69.8 ± 6.9	56.0–83.6
D33	21.6 m	1.47 ± 0.015	7.49 ± 0.02	1.792	11.7 ± 5%	2.64 ± 0.20	164.72 ± 29.44	62.4 ± 12.1	38.2–86.6
D34	22.2 m	1.51 ± 0.015	7.55 ± 0.02	1.536	13.6 ± 5%	2.37 ± 0.18	174.43 ± 8.49	73.7 ± 6.6	60.5–86.9
D37	25.3 m	1.96 ± 0.015	9.30 ± 0.02	1.824	13.6 ± 5%	2.88 ± 0.21	286.52 ± 18.22	99.5 ± 9.8	79.9–119.1
D38	25.5 m	1.51 ± 0.015	7.32 ± 0.02	1.672	15.2 ± 5%	2.41 ± 0.18	218.49 ± 12.55	90.8 ± 8.6	73.6–108.0

Note: *The age included one standard deviation of the OSL measurements. **Confident intervals of radiocarbon date at 95.4% confident level.

Please cite this article as: Yi, L., et al., Late Quaternary linkage of sedimentary records to three astronomical rhythms and the Asian monsoon, inferred from a coastal boreho..., Palaeogeogr. Palaeoclimatol. Palaeoecol. (2012), doi:10.1016/j.palaeo.2012.02.020

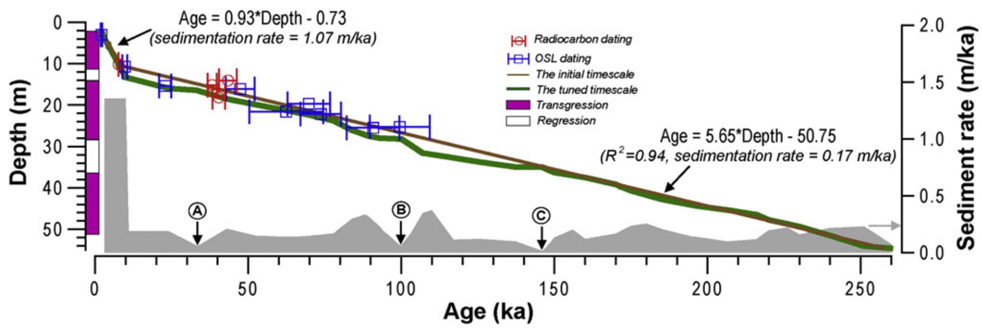

Fig. 7. Timescale comparison between the chronologies based upon absolute dating and astronomical tuning. The sedimentation rate changes (grey-shadow area) and the possible three hiatuses (labeled A, B and C) according to the astronomical chronology are also displayed. See details in text.

width of 10–15 km. During a regression, though the rivers could extend further into the Laizhou Bay where the water depth is less than 15 m (IOCAS, 1985), the stream gradient or the average slope would not change substantially, implying that the dominant factor of flow velocity is not stream gradient, but water discharge: when the water discharge increases, the flow velocity would enlarge and the re-suspension strengthen.

An empirical relationship between water discharge (Q_R, m^3/s) and regional precipitation (r, mm/a) can be expressed as follows (Kjerfve, 1990):

$$Q_R = \int\int r \times e^{-\frac{E_0}{r}} dA$$

where dA is each drainage basin (km^2), and E_0 is a potential evapotranspiration (mm/a). The equation indicates that water discharge is linked to regional precipitation in a strong and positive relation: when the regional precipitation increases, the water discharge rises. Furthermore, a positively linear association between water discharge and sediment loads is also reported from the western slopes of the Columbian Andes (Restrepo and Kjerfve, 2000), the five ephemeral streams in Wyoming in the USA (Rankl, 2004) and the Pearl River in China (Zhang et al., 2007).

The local drainage system at our location includes mainly the Xiaoqinghe River, Mihe River and Weihe River. The association (Fig. 8) of water discharge with the amount of suspended materials of these local rivers is $r = 0.82$ ($p < 0.01$), and with regional precipitation is $r = 0.91$ ($p < 0.01$).

Given that the regional precipitation is predominantly controlled by the Asian monsoon, we infer that the GS series is essentially an indicator of Asian monsoon intensity: when the Asian monsoon strengthens, regional precipitation increases, the water discharge of local rivers increases, the amount of re-suspended materials ascends, and the GS values enlarge.

5.2. Astronomical timescale based on the GS series

Because the Asian monsoon is dominated by orbital changes (An et al., 1990; Cheng et al., 2009; Guo et al., 1998; Liu and Ding, 1993; Liu and Ding, 1998; Porter and An, 1995; Sun et al., 2006, 2012; Wang et al., 2001, 2005, 2008) and because the GS series indicates the variability of Asian monsoon intensity, which responds to solar insolation (Cheng et al., 2009; Wang et al., 2001, 2008) at precessional periodicities (Fig. 9), it is possible to refine the preliminary timescale using the orbital tuning. This approach has been widely used to construct age models for deep sea sediments (Ao et al., 2011; Hüsing et al., 2010; Lisiecki and Raymo, 2005; Ruddiman et al., 1989; Tian et al., 2008), Chinese loess (Ding et al., 1994; Lu et al., 1999; Sun et al., 2006), and other continental deposits (An et al., 2011; Aziz et al., 2003; van Vugt et al., 1998).

5.2.1. Tuning target curve

For the construction of an astronomical timescale, the selection of suitable target curves is crucial. In this study, we selected the 65 N summer insolation (Berger and Loutre, 1991) for the tuning of Lz908 core, because it is a major forcing factor for Asian monsoon on the orbital timescales (An et al., 2001; Cheng et al., 2009; Guo et al., 2002; Wang et al., 2001, 2005, 2008). Additionally, the solar radiation estimated at latitude 65 N was the original forcing function and has long been regarded as a typical indication for Northern Hemisphere radiation conditions (e.g. Berger and Loutre, 1991; Imbrie et al., 1984; Paillard, 1998).

As proposed by Ruddiman (2006), the Asian monsoon should respond to the Northern Hemisphere summer insolation with a near-zero phase lag, and this is supported from the phase relationship between the Chinese stalagmite $\delta^{18}O$ series and solar insolation over the past ~400 ka (Cheng et al., 2009; Wang et al., 2008). Thus, we assumed no phase difference existed between the solar insolation curves and the monsoon climate response throughout the last 260 ka.

5.2.2. Orbital tuning

First, the GS series and the 65 N latitude summer solar insolation time series (Berger and Loutre, 1991) were visually matched (Fig. 9). Then the GS time series was filtered using a band-pass filter centered on the precession frequency (19–23 ka), and the resulting curves were correlated with the unfiltered solar insolation time series. Additional age control points were added iteratively until the unfiltered GS time series and the solar radiation time series showed a good match, as confirmed by cross spectral coherence (Fig. 9). We used a cubic spline interpolation technique on the additional age

Table 3
Hiatuses reported in the west Bohai Sea, China.(1).

No.	Depth	Position	Lasting	Number of cores
Hiatus-1	10 m	Middle of T-1	1 ka	6
Hiatus-2	16 m	Beginning of T-1	8 ka	6
Hiatus-3	25 m	End of T-2	3 ka	2 (3)
Hiatus-4 (2)	41 m	Beginning of T-2	–	1 (3)
Hiatus-5	80 m	Beginning of T-3	-	1 (3)

Note: (1) This table was re-plotted from Li et al. (2004) based on six boreholes drilled in the west Bohai Sea, China. (2) Hiatus-4 represents a period with low sedimentation rate. (3) These hiatuses were only observed in the cores located in the coastal plain of west Bohai Sea, China.

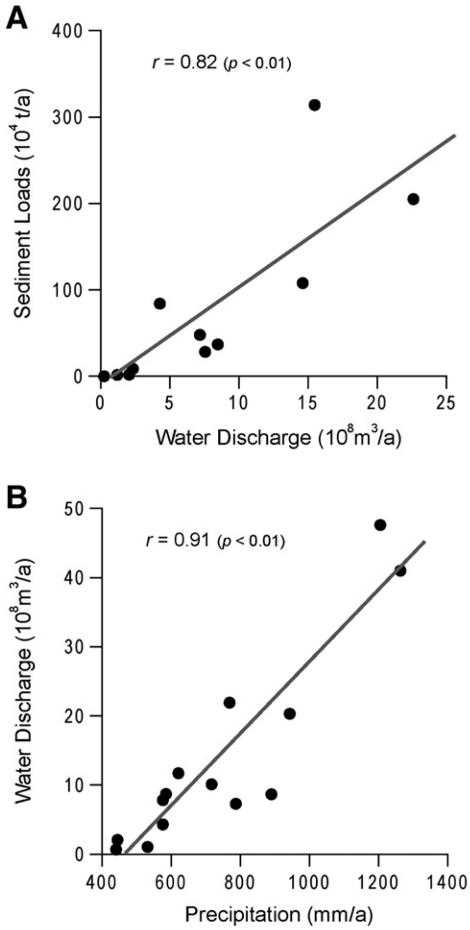

Fig. 8. A, the relationship between sediment loads and water discharge of the Xiaoqinghe River, Mihe River and Weihe River (data from SDSTC, 1990). B, the relationship between water discharge and catchments precipitation of the Xiaoqinghe River, Mihe River and Weihe River (data from Cao et al., 1998).

points to improve covariance of the GS and the insolation time series (Ding et al., 1994; Lu et al., 1999). When tuning the time scale for the GS series, we also referred to the Asian monsoon intensity integrated from the stalagmite $\delta^{18}O$ series in Hulu Cave and Sanbao Cave (Cheng et al., 2009; Wang et al., 2001, 2008) to assist in matching the short climatic variations.

5.2.3. Testing the new timescale and refined rate of sediment accumulation

In order to test the coherency between our GS on the new chronology and the insolation time series, spectral analyses were conducted (Fig. 9). Results indicate that during the period 2–260 ka, on the precessional periodicities, i.e. 19–23 ka, the coherency is significant and over the 5% significance level. The correlation coefficient between the insolation time series and the filtered GS variation at the precession band (19–23 ka) was also improved from $r = 0.43$ to $r = 0.90$ through the orbital tuning processes.

The sedimentation rate derived from the tuned age model is similar to that derived from the initial age model (Fig. 7). The sedimentation rate in the Holocene was 1.35 m/ka which is slightly higher than that from the initial age model, and in the pre-Holocene averaged 0.17 m/ka ranging between 0.02 and 0.37 m/ka. Low sedimentation rates (0.02–0.05 m/ka) were observed at depths of 16.6 m (34 ka), 28.2 m (100 ka) and 35 m (145 ka), which correspond to the end of T-2, beginning of T-2 and during the regression 2 (Fig. 7). The changing pattern of sediment accumulation rate was somewhat similar to that of Li et al. (2004) for the west Bohai Sea, China, indicating low sedimentation rates during only a few intervals in the past 260 ka. Furthermore, these periods were millennial but not orbital, and their existence would not essentially affect the reliability of the astronomically tuned timescale.

6. Results

The most noticeable feature of these coastal sediment variations is the little similarity in pattern between the three proxies (Figs. 2, 3, 10), i.e. GS, MS series and tree-pollen abundance, but greater similarity between GS and the Chinese stalagmite $\delta^{18}O$ series (Cheng et al., 2009; Wang et al., 2001, 2008) and July insolation at 65 N (precession cycles, determining the season when the Earth is closest to the Sun; Berger and Loutre, 1991), between MS and obliquity changes (tilt of rotational axis, determining the meridional gradient in insolation), and between tree-pollen abundance and deep sea sediment $\delta^{18}O$ records (Lisiecki and Raymo, 2005) and eccentricity change (determining the semi-annual difference in distance to the sun), respectively (Fig. 10). Little internal similarity between records compared with high similarity with external records indicates that the coastal sediments in the south Bohai Sea integrate different influences from various environmental factors.

(1) For the GS series, it indicates Asian monsoon intensity. When the Asian monsoon strengthens, regional precipitation increases, the water discharge of local rivers increases, the amount of re-suspended materials increases, and the GS values rise; but when the Asian monsoon weakened, the GS values decrease.
(2) For the MS series, it seems that this proxy was regulated by orbital tilt with a phase lag of 8–12 ka relative to obliquity minima. During the periods of low obliquity, the coastal sediments displayed low magnetic susceptibility values, but under contrary conditions, the MS values were high.
(3) For vegetation cover, although it was difficult to determine the exact phase lag of vegetation to global ice volume because of its low resolution, tree-pollen abundance seems, apparently, to be driven by global ice volume. When the global ice extended, the annual temperature was low, the EAWM strengthened and the regional arboreal vegetation coverage was limited; and when the global ice volume declined, the annual temperature became high, the EAWM weakened and the regional arboreal vegetation expanded.

MTM spectral analysis (Dettinger et al., 1995; Ghil et al., 2002) confirms these orbital relationships in dominance (Fig. 11): 19–23-ka periodicity shows the highest power in GS, 41-ka period in the MS series, and the 100-ka periodicity in the tree-pollen component.

7. Discussions

7.1. Driving force of the Asian monsoon

Based upon the GS variability and its spectrum (Figs. 9, 10, 11), we inferred that the Asian monsoon variability recorded in the Bohai Sea was dominated by solar insolation rather than ice volume changes: when the solar insolation was high, the ITCZ moved northward resulting in more moisture transported to the Asian inland area. This is consistent with many low-latitude studies (e.g. Ao et al., 2011; Cheng et al., 2009; Wang et al., 2001, 2005, 2008). However, the complexity arises in that the ~100-ka cycles were also observed in the GS spectrum (Fig. 11A) indicating some possible influence from the global ice volume changes. These ~100-ka cycles were also broadly reported in inland-related records (e.g. Liu, 1985; Kukla, 1987; An et al., 1990, 2001, 2011; Liu and Ding, 1993; Ding et al., 1995; Liu et al., 1999; Wang et al., 1999; Wehausen and Brumsack, 2002; Sun et al., 2006, 2012). Thus, as suggested by Wang (2009), we propose that the Asian monsoon variability

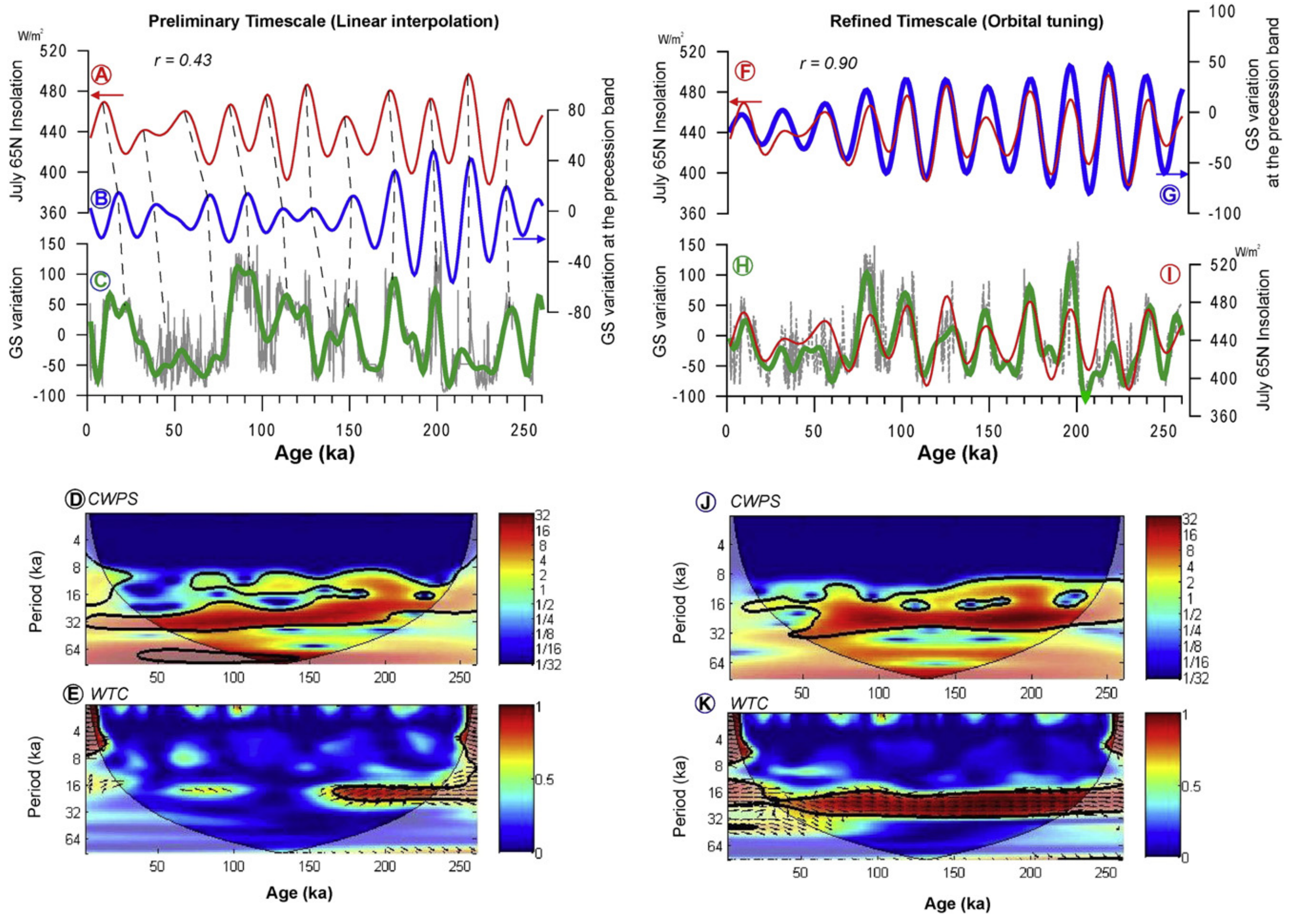

Fig. 9. Testing the astronomical tuning chronology of Lz908 core. A, F and I (red thin lines), are the July solar insolation at 65 N (Berger and Loutre, 1991). B and G (blue bold lines) are the GS variability at 19–23 ka band. C and H are the original (grey dash lines) and low-frequency variation (>10 ka, FFT filter, bold lines) of GS series. D and J are the continuous wavelet power spectrum (CWPS, Grinsted et al., 2004) of the filtered variation of the GS series (FFT filter, f<0.1). The thick black contour designates the 5% significance level against red noise and the cone of influence (COI) where edge effects might distort the picture is shown as a lighter shade. E and K are the squared wavelet coherence (WTC, Grinsted et al., 2004) between the filtered GS variation (this study) and the July solar insolation at 65 N (Berger and Loutre, 1991). The 5% significance level against red noise is shown as a thick contour. All significant sections show in-phase behavior (with in-phase pointing right, anti-phase pointing left). All the plots in the left panel represent the results based on the initial timescale, and the plots in the right panel represent the results from orbital tuning. (For interpretation of the references to color in this figure legend, the reader is referred to the web version of this article.)

recorded in the Bohai Sea demonstrates the interaction between the internal (global ice volume) and external (solar insolation) factors, but the external factor (solar insolation) was the predominant one.

7.2. Magnetic susceptibility vs. obliquity changes

The MS value is determined by the amount of magnetic grains carried from the sediment source and the pedogenetic intensity after settlement. Mineral investigation under the microscope shows that there are only two kinds of magnetic minerals present: the major is ilmenite and the minor is limonite (Yi, 2010). As the Luzhong Mountain Range is renowned for the production of ilmenite, it is inferred that the pedogenetic intensity was weak and the source of magnetic mineral was the controlling factor in the MS variation.

The local rivers to the south Bohai Sea carried the magnetic grains, and these grains were a result of river incision around the sediment's source. A classical model of fluvial sedimentation in response to climate change is described as follows (Vandenberghe, 1995, 2003): during the glacial stages, due to the catchment's erosion enhanced by limited vegetation, the sediment supply to the rivers increases, while higher temperature and more humid interglacials result in denser vegetation and a reduction in sediment supply; and an incision takes place at the climate transitions, when the river system becomes unstable. We described the link here, between MS and climate changes, as a result of enhanced incision during the climate transitions providing more magnetic grains into the rivers flowing into the south Bohai Sea.

A statistical test of the ice terminations suggested that the orbital tilt paced the deglaciations, and, since the mid-Pleistocene, the climate state has skipped one or two obliquity beats, thus giving glacial-cycle durations of ~100 ka (Huybers and Wunsch, 2005). Because at the beginning of glaciations the basal temperature was low (Marshall and Clark, 2002), the obliquity pacing had little effect on the ice melting (Huybers and Wunsch, 2005), but when the ice sheets became thick, the increased obliquity caused increasing high-latitude insolation and ice sheet melting (Huybers and Wunsch, 2005) coupled with high basal temperature and pressure (Marshall and Clark, 2002). Because a lag of ~10 ka is required for surface heating to ice sheets (Marshall and Clark, 2002), the observed 8–12 ka lags of MS to the obliquity pacing could be a response to this heat transfer process.

The condition in the south Bohai Sea would be somewhat different, because it is located on marginal areas of the Arctic and Siberian ice sheets. While the question of whether glaciations occurred during the late Quaternary in the eastern China (e.g. Kusky et al., 2011; Lee, 1933,1934, 1936; Li et al., 2008; Lü et al., 2010; Zhao, 2010) or did not (e.g. Shi et al., 1987; Shi, 2000, 2010; Zhou, 2006), is still hotly debated, the study area did experience an extremely cold

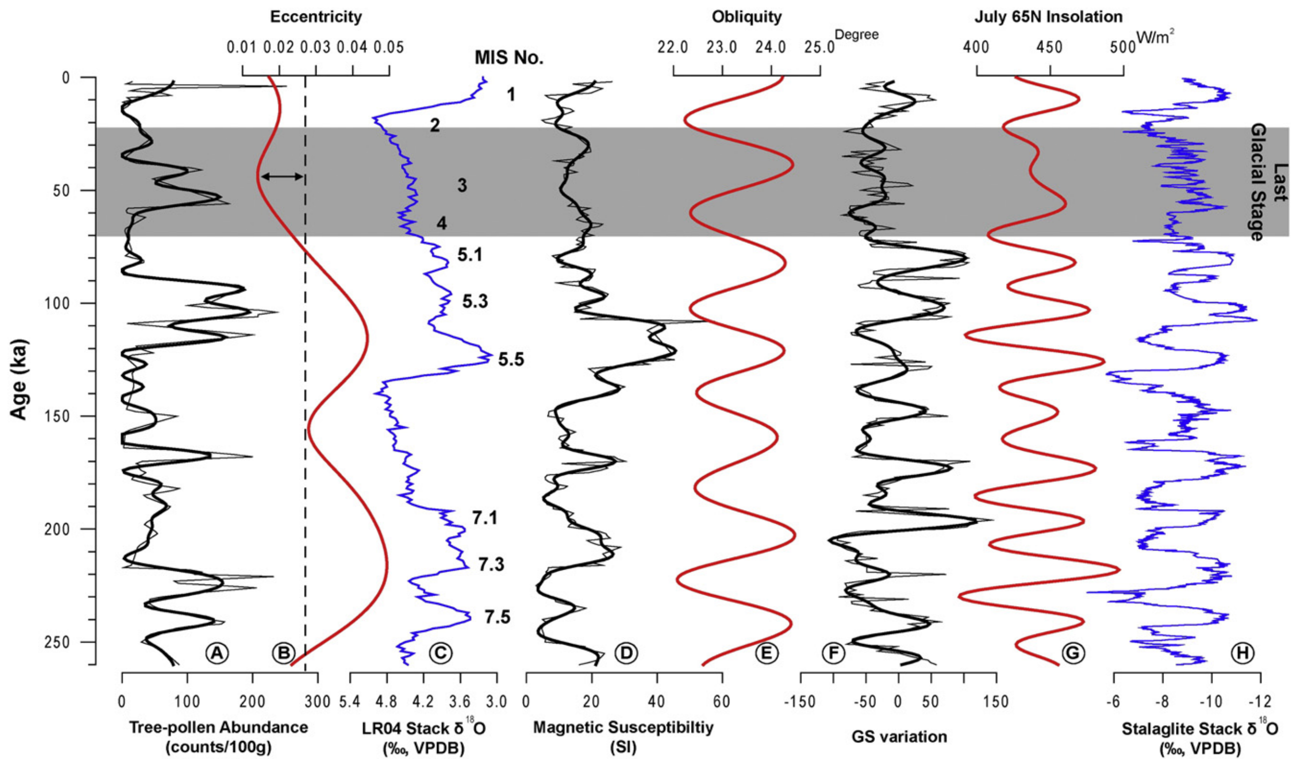

Fig. 10. Tree-pollen abundance (A), MS series (D) and GS series (F) are three proxies developed in this research (thin lines are plotted from original data and bold lines from FFT filtered data at $f<0.1$). Eccentricity (B), orbital tilt with 8-ka lead (E) and July insolation at 65°N (G) — the orbital changes involved in the comparison (Berger and Loutre, 1991). (C) Deep sea sediment $\delta^{18}O$ records (LR04 stack, Lisiecki and Raymo, 2005). Marine isotopic stages labeled. (H) Stalagmite $\delta^{18}O$ series integrated from Hulu Cave and Sanbao Cave (Cheng et al., 2009; Wang et al., 2001, 2008). All series plotted here were interpolated at 1-ka temporal interval. See details in text.

environment in that wooly rhinoceros and mammoth fossils from this time period have been found around the Bohai Sea (IOCAS, 1985). Because the latitude of the Bohai Sea is lower than the Arctic and Siberian ice sheets and closer to the Pacific Ocean, it seems that the heat and moisture transported from the low-latitude ocean could have more efficiently reached the study area. Thus, we speculate that in study area obliquity pacing may be more sensitive to heat and moisture transferred from the proximal ocean: during periods with greater obliquity, the enhanced meridional insolation gradient would enhance heat and moisture transport from low- to high-latitude than during the period with less obliquity. In this process, the obliquity heating could liberate the study area from an extremely cold environment and potentially increase climatic variation. The climate transition has caused strengthening of incision processing, allowing more magnetic materials to flow to the south Bohai Sea. Thus, we employed this mechanism to explain the relationship between the MS series and the obliquity pacing.

7.3. Vegetation coverage vs. global ice volume

The vegetation coverage indicated from the tree-pollen abundance could be controlled by the vegetation distribution in a glacial stage when the continental shelves were exposed or the regional humidity changes (Sun et al., 2003). To identify the dominant factor, the principle of limiting factors, which states that tree growth is limited by various environmental factors, would be helpful. The principle of limiting factors was proposed that (Fritts, 1976): (1) in arid areas, tree growth can not proceed faster than that allowed by the amount of precipitation, causing tree volume to be a function of precipitation; (2) at higher latitudes and elevations, temperature is often the most limiting factor; and (3) for many forest trees, especially those growing in temperate and/or closed canopy conditions, the most limited factors are the processes related to stand dynamics (especially competition for nutrients and light) rather than climatic changes.

The tree-pollen in the south Bohai Sea mainly comes from the Luzhong Mountain Range (Zhang et al., 2008b), which is presently a semi-humid or humid area. However, during a glacial stage, the exposed Bohai Basin might have been covered by part of diluvia fan (Chen et al., 1991), loess/sandy dune (Chen et al., 1991; Yu et al., 1999; Zhao, 1991, 1995) or alluvial fan (Meng et al., 1999), lacking forest. Thus, it is inferred that both the hydrological conditions and the vegetation distribution changes were not the limited factors.

Temperature has been shown to be an important factor in tree growth and forest ecosystem dynamics (e.g. Briffa et al., 2001; Buckley et al., 1997; Jacoby and D'Arrigo, 1989; Kullman, 2001; Villalba, 1994). Biological study of tree-ring radial growth on the northern range margin of the United States showed that winter temperature could most limit growth at the ecosystem level (Pederson et al., 2004), supporting the hypothesis that winter temperatures may control vegetation ecotones. The reconstructed mean temperature of both warmest and coldest months, which were extracted from lacustrine sediment pollen data in Lake Biwa, Japan, showed great consistency with global ice volume (Nakagawa et al., 2008). Moreover, Liu et al. (2010) also reported in the Luzhong Mountain Range the predominant influence of annual minimum temperature on tree growth. This implies that temperature has a predominant effect on regional vegetation change.

The global temperature has changed with global ice volume in a dominant periodicity of ~100 ka during the past ~800 ka (e.g. Lisiecki and Raymo, 2005). The tree-pollen abundance approximately matches the evolution patterns of global temperatures, indicating consistency between regional and global changes and demonstrating fidelity of the orbital tuning process.

7.4. Complex linkages to astronomical forcing

However, complexity is inherent in paleoenvironmental changes and its driving processing. Although the three paleoenvironmental proxies developed here relate to different controlling processes

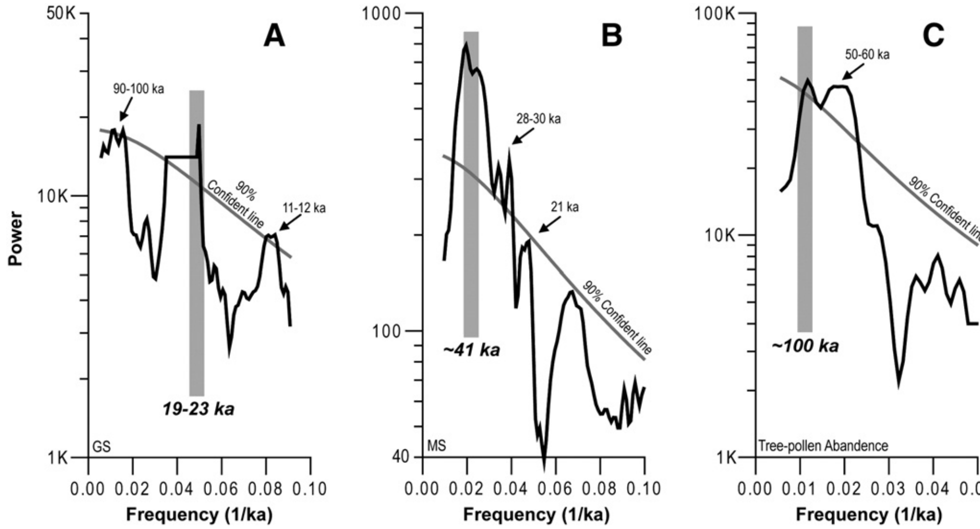

Fig. 11. The multi-taper method (MTM) of spectral analysis (Dettinger et al., 1995; Ghil et al., 2002) for the GS (A), MS (B) and tree-pollen abundance (C). The significant periodicities are labeled.

operating at distinct periodicities, all the three variations on orbital timescales exhibit the influence of a predominant astronomical periodicity and one or more recessive periodicities (Fig. 12). For example, in the spectral analysis (Fig. 11), recessive components of 100-ka cycles existed in the GS series, of precessional cycles in the MS series and of 50–60-ka cycles (obliquity cycles, Berger and Loutre, 1991) in the tree-pollen abundance.

(1) The GS variation was dominated by precessional cycles with a slight 100-ka component indicating a combination between solar insolation and global ice volume changes. The linkage from the global ice volume changes to GS variability was probably, as previous mentioned, related to: (a) the global sea levels that decreased the distance between continent and ocean reducing the heat and moisture transported inland (Wang, 1999); (b) the decreased sea surface temperature likely reduced the evaporation and the transported moisture (Guo et al., 2002, 2004); and (c) the strengthened Siberian–Mongolian Highs increased the winter monsoon and reduced the heat and moisture carried from the ocean (Ding et al., 1994).

(2) The MS variation, associated with river incision in the sediment source area, responded to the obliquity pacing, because the magnetic materials eroded from the Luzhong Mountain Range were carried by local rivers to the south Bohai Sea. Because the water discharge was related to the Asian Monsoon variability, during the sediment transport, the precessional cycles are likely to have been transferred into the MS series and expressed as precessional cycles in the MS spectrum. Additionally, if there were frequent large floods in some periods as suggested by Shi and Deng (1982) and Shi (2010), river incision would also have

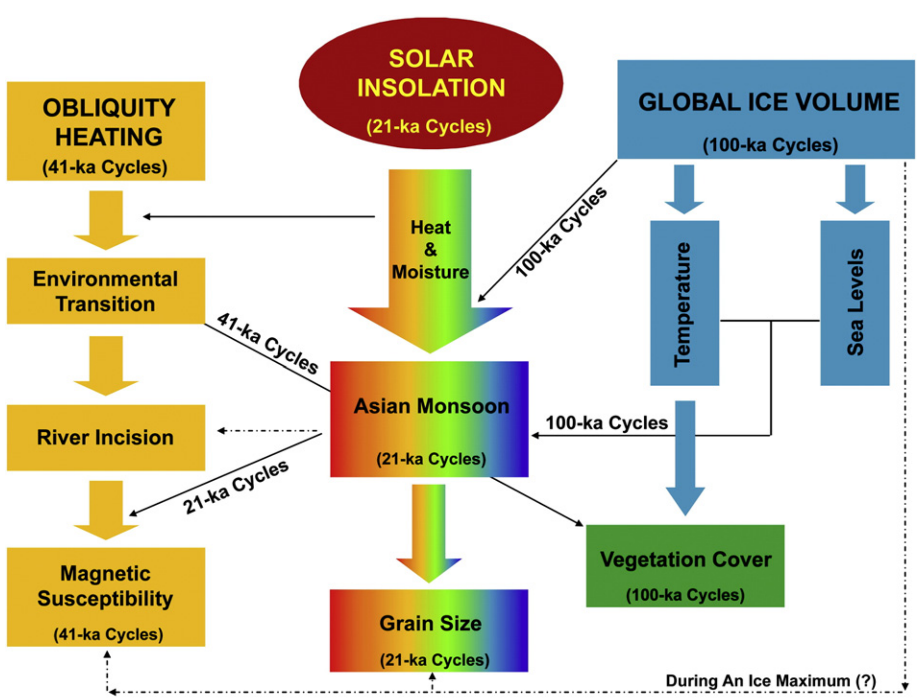

Fig. 12. Complex linkages between sedimentary records in the south Bohai Sea, China and Asian monsoon and three astronomical rhythms. See details in text.

been enhanced and the 41-ka cycles disturbed. We assumed that these processes might have transferred the precessional cycles into the MS variation.

(3) The temperature condition was not only related to global ice volume but also climatic changes in the source area. Because climatic transitions in the Luzhong Mountain Range occur nearly every obliquity pacing, these accelerated climatic transitions possibly affected the vegetation recovery process. Because the 50–60 ka cycles are components of obliquity changes (Berger and Loutre, 1991), the obliquity cycles might be transferred into the tree-pollen abundance variation.

(4) During the last glacial stage, the three proxies waxed and waned with less amplification than during MIS 7–6 (Fig. 10), probably indicating the eccentricity cycles have over-ridden the influences of precession and orbital tilt. Even though eccentricity has little direct impact on insolation, it has a large indirect impact on climate through its modulation of orbital precession (Ruddiman, 2006). When the amplitude of orbital forcing falls below a threshold level, the eccentricity cycle would dominate Asian monsoon intensity (Nakagawa et al., 2008). However, the last glacial stage is a period of eccentricity minimum during the last 260 ka (Fig. 10). During this period, global ice volume extended over an extremely large level, the very low global sea levels caused exposure of the mainly continental shelf of the west Pacific (Liu, 2009), and the Asian continent became nearly twice as remote from maritime influences (Nakagawa et al., 2008). Thus, all the controlling effect of precession and obliquity pacing weakened, and three proxies were expressed in 100-ka cycles.

Therefore, neither external nor internal factors could dominate the paleoenvironmental evolution on orbital timescales in a separated way, and they are both integrated in a complex pattern (Fig. 12). Every dominant or recessive factor, even with small changes, could possibly have fingerprints in the paleoenvironmental evolution and imprinted their periodicities significantly on the proxies, demonstrating the nonlinear processes and the complex inherence.

8. Conclusions

To study the late Quaternary coastal evolution in the south Bohai Sea, a new borehole, Lz908, was drilled. Three proxies, i.e. grain size, magnetic susceptibility and tree-pollen abundance, were investigated to construct regional environment changes. The most noticeable feature was that the three proxies had various dominant factors, including Asian monsoon intensity, obliquity pacing and global ice volume.

The linkages of these proxies to the dominant forcing factors are proposed, and the main conclusions are: (1) grain size variability is an indicator of the Asian monsoon intensity, which is dominated by both solar insolation (major) and global ice volume (minor) forcing; (2) the magnetic susceptibility variation was sensitive to orbital tilt through river incision processes coupled to solar insolation; (3) the vegetation coverage responded to temperature variation which is subjected to global ice volume with influence from obliquity changes; (4) While all proxies exhibited a predominant periodicity, the presence of minor periodicities arising from other orbital periods has indicated the complexity of the natural system. These linkages confirmed that the sedimentary records in the south Bohai Sea, China, record the nonlinear processes and the complex inherence in paleoenvironmental evolution and driving processing.

Acknowledgements

The authors thank Prof. Peter Kershaw (Editor) and two anonymous reviewers for their suggestion and comments in improving this manuscript. Dr. Haijun Huang in Institute of Oceanology, CAS, provided the surface sediment samples. Prof. Zhiwei Yu in China University of Mining and Technology provided the orbital tuning program. We wish to thank Prof. Songling Zhao in Institute of Oceanology, CAS; Dr. Zhongping Lai in Qinghai Institute of Salt Lake, CAS; Drs. Liangcheng Tan, Hai Xu and Shugang Kang in Institute of Earth Environment, CAS; Dr. Xin Zhou in University of Science and Technology of China and Drs. Zhengquan Yao, Qiao Su, Guangquan Chen and Yuanqin Xu in First Institute of Oceanography, SOA for their valuable advice, comments and discussion. Prof. Daniel Kister proofread the early edition of manuscript. Dr. Qiang Chen and Ms. Wenqin Zhang provided help in OSL measurements and pollen identification, respectively. This research was supported by National Basic Research Project of China (grant: 2010CB951200), State Oceanic Research Project for Public Benefit (grant: 201105020, 200805063), Chinese Offshore Investigation and Assessment (grant: 908-01-ZH2) and State Key Laboratory of Loess and Quaternary Geology of China (grant: SKLLQG1018).

References

Aitken, M.J., 1998. An Introduction to Optical Dating, 2 edition. Oxford University Press, p. 279.

An, Z.S., Liu, T.S., Lu, Y.C., Porter, S.C., Kukla, G., Wu, X.H., Hua, Y.M., 1990. The long-term palaeomonsoon variation recorded by the loess–paleosol sequence in central China. Quaternary International 7 (8), 91–95.

An, Z., Kukla, G.J., Porter, S.C., Xiao, J., 1991. Magnetic susceptibility evidence of monsoon variation on the Loess Plateau of central China during the last 130,000 years. Quaternary Research 36, 29–36.

An, Z.S., Kutzbach, J.E., Prell, W.L., Porter, S.C., 2001. Evolution of Asian monsoons and phased uplift of the Himalaya–Tibetan plateau since late Miocene times. Nature 411, 62–66.

An, Z.S., Clemens, S.C., Shen, J., Qiang, X., Jin, Z., Sun, Y., Prell, W.L., Luo, J., Wang, S., Xu, H., Cai, Y., Zhou, W., Liu, X., Liu, W., Shi, Z., Yan, L., Xiao, X., Chang, H., Wu, F., Ai, L., Lu, F., 2011. Glacial–interglacial Indian summer monsoon dynamics. Science 333, 719–723.

Ao, H., Dekkers, M.J., Qin, L., Xiao, G.Q., 2011. An updated astronomical timescale for the Plio-Pleistocene deposits from South China Sea and new insights into Asian monsoon evolution. Quaternary Science Reviews 30, 1560–1575.

Aziz, H.A., Krijgsman, W., Hilgen, F.J., Wilson, D.S., Calvo, J.P., 2003. An astronomical polarity timescale for the late middle Miocene based on cyclic continental sequences. Journal of Geophysical Research 108, 2159.

Barbetti, M.F., McElhinny, M.W., 1976. The Lake Mungo geomagnetic excursion. Philosophical Transactions of the Royal Society A 281, 515–542.

Berger, A., Loutre, M.F., 1991. Insolation values for the climate of the last 10 million - years. Quaternary Science Reviews 10, 297–317.

Boulay, S., Colin, C., Trentesaux, A., Clain, S., Liu, Z.F., Lauer-Leredde, C., 2007. Sedimentary responses to the Pleistocene climatic variations recorded in the South China Sea. Quaternary Research 68, 162–172.

Briffa, K.R., Osborn, T.J., Schweingruber, F.H., Harris, I.C., Jones, P.D., Shiyatov, S.G., Vaganov, E.A., 2001. Low-frequency temperature variations from a northern tree ring density network. Journal of Geophysical Research 106, 2929–2941.

Buckley, B.M., Cook, E.R., Peterson, M.J., Barbetti, M.F., 1997. A changing temperature response with elevation for *Lagarostrobos franklinii* in Tasmania, Australia. Climatic Change 36, 477–498.

Campbell, C., 1998. Late Holocene lake sedimentology and climate change in Southern Alberta, Canada. Quaternary Research 49, 96–101.

Cao, S.L., Yu, C.S., Sun, X.L., 1998. Methodology study of identifying the maximum and minimum values in annual series of precipitation and water discharge. Journal of China Hydrology 22–26 (In Chinese).

CDIG (Shaanbei Team, Chengdu Institute of Geology), 1978. The grain-size analysis and its application of sedimentary rocks. Geology Press, Beijing. 147 pp. (In Chinese).

Chao, W.C., Chen, B.D., 2001. The origin of monsoons. Journal of the Atmospheric Sciences 58, 3497–3507.

Chappell, J., Omura, A., Esat, T., McCulloch, M., Pandolfi, J., Ota, Y., Pillans, B., 1996. Reconciliation of late Quaternary sea levels derived from coral terraces at Huon Peninsula with deep sea oxygen isotope records. Earth and Planetary Science Letters 141, 227–236.

Chen, B.A., 1982. Characteristics of sediment dynamics around the Xiaoqinghe Estuary. Marine Science Bulletin 1, 57–70 (In Chinese).

Chen, M., Chen, J.G., Wang, J.F., 1991. The evolution trend of swamping, salting and desertization along the coast of Bohai Sea and its relationship to global change. Quaternary Sciences 11, 113–122 (In Chinese).

Chen, Y.K., Li, Z.H., Shao, Y.X., Wang, Z.S., Gao, W.P., Yang, X.L., 2008. Study on the Quaternary chronostratigraphic section in Tianjin Area. Seismology and Geology 30, 383–399 (In Chinese with English Abstract).

Chen, B., Huang, H.-J., Mei, B., 2009. Characteristics of sediment transportation near Xiaoqing Estuary. Marine Geology & Quaternary Geology 29, 35–42 (In Chinese with English Abstract).

Cheng, H., Edwards, R.L., Broecker, W.S., Denton, G.H., Kong, X., Wang, Y., Zhang, R., Wang, X., 2009. Ice age terminations. Science 326, 248–252.

Clemens, S.C., Prell, W.L., 2003. A 350,000 year summer–monsoon multi-proxy stack from the Owen Ridge, Northern Arabian Sea. Marine Geology 201, 35–51.

Clemens, S.C., Prell, W.L., Murray, D., Shimmield, G., Weedon, G., 1991. Forcing mechanisms of the Indian Ocean monsoon. Nature 353, 720–725.

Clemens, S.C., Prell, W.L., Sun, Y.B., 2010. Orbital-scale timing and mechanisms driving Late Pleistocene Indo-Asian summer monsoons: reinterpreting cave speleothem d18O. Paleoceanography 25, PA4207.

Cook, E.R., Anchukaitis, K.J., Buckley, B.M., D'Arrigo, R.D., Jacoby, G.C., Wright, W.E., 2010. Asian monsoon failure and megadrought during the Last Millennium. Science 328, 486–489.

Darby, D.A., Ortiz, J.D., Polyak, L., Lund, S., Jakobsson, M., Woodgate, R.A., 2009. The role of currents and sea ice in both slowly deposited central Arctic and rapidly deposited Chukchi–Alaskan margin sediments. Global and Planetary Change 68, 58–72.

Dettinger, M.D., Ghil, M., Strong, C.M., Weibel, W., Yiou, P., 1995. Software expedites singular-spectrum analysis of noisy time series. EOS. Transactions of the American Geophysical Union 76, 12, 14, 21.

Ding, Z.L., Yu, Z.W., Rutter, N.W., Liu, T.S., 1994. Towards an orbital time scale for Chinese loess deposits. Quaternary Science Reviews 13, 39–70.

Ding, Z.L., Liu, T.S., Rutter, N.W., Yu, Z.W., Guo, Z.T., Zhu, R.X., 1995. Ice-volume forcing of East Asian winter monsoon variations in the past 800,000 years. Quaternary Research 44, 149–159.

Du, T.Q., Huang, H.J., Yan, L.W., Liu, G.W., Song, Z.J., 2008. Characteristics of suspended matters in winter water off the Xiaoqinghe River estuary. Marine Geology & Quaternary Geology 28, 41–48 (In Chinese with English Abstract).

Fritts, H.C., 1976. Tree Ring and Climate. Academic Press, London. 567 pp.

Gao, W.M., Li, J.L., Sun, Z.Y., 1980. Formation and evolution of the Yi-Shu continental rift. Seismological Geology 2, 11–18.

Gao, X., Wang, Q., Li, Y., Du, N., Kong, Z., 1986. Transgressive and paleoclimatic comparison since late mid-Pleistocene, inferred from the Borehole P8 in the Tianjin Area. Marine Geology & Quaternary Geology 6, 53–64 (In Chinese with English Abstract).

Ghil, M., Allen, M.R., Dettinger, M.D., Ide, K., Kondrashov, D., Mann, M.E., Robertson, A.W., Saunders, A., Tian, Y., Varadi, F., Yiou, P., 2002. Advanced spectral methods for climatic time series. Reviews of Geophysics 40, 1003.

Grinsted, A., Moore, J.C., Jevrejeva, S., 2004. Application of the cross wavelet transform and wavelet coherence to geophysical time series. Nonlinear Processes in Geophysics 11, 561–566.

Guo, Z., Liu, T., Fedoroff, N., Wei, L., Ding, Z., Wu, N., Lu, H., Jiang, W., An, Z., 1998. Climate extremes in Loess of China coupled with the strength of deep-water formation in the North Atlantic. Global and Planetary Change 18, 113–128.

Guo, Z.T., Ruddiman, W.F., Hao, Q.Z., Wu, H.B., Qiao, Y.S., Zhu, R.X., Peng, S.Z., Wei, J.J., Yuan, B.Y., Liu, T.S., 2002. Onset of Asian desertification by 22 Myr ago inferred from loess deposits in China. Nature 416, 159–163.

Guo, Z.T., Peng, S.Z., Hao, Q.Z., Biscaye, P.E., An, Z.S., Liu, T.S., 2004. Late Miocene–Pliocene development of Asian aridification as recorded in the Red-Earth Formation in northern China. Global and Planetary Change 41, 135–145.

Han, Y.S., Meng, G.L., Wang, S.Q., 1994. The geological events and paleo-environment of the coastal plain of Laizhou Bay in Bohai Sea during late Quaternary. Studia Marine Sinica 35, 87–96 (In Chinese with English Abstract).

Hao, Q.Z., Oldfield, F., Bloemendal, J., Guo, Z.T., 2008. Particle size separation and evidence for pedogenesis in samples from the Chinese Loess Plateau spanning the last 22 Ma. Geology 36, 727–730.

Hüsing, S.K., Cascella, A., Hilgen, F.J., Krijgsman, W., Kuiper, K.F., Turco, E., Wilson, D., 2010. Astrochronology of the Mediterranean Langhian between 15.29 and 14.17 Ma. Earth and Planetary Science Letters 290, 254–269.

Huybers, P., Wunsch, C., 2005. Obliquity pacing of the late Pleistocene glacial terminations. Nature 434, 491–494.

Imbrie, J., Hays, J.D., Martinson, D.G., McIntyre, A., Mix, A.C., Morley, J.J., Pisias, N.G., Prell, W.L., Shackleton, N.J., 1984. The orbital theory of Pleistocene climate: support from a revised chronology of the marine d18O record. In: Berger, A.L., et al. (Ed.), Milankovitch and Climate, Part I. D. Reidel, Dordrecht, pp. 269–305.

IOCAS (Marine Geology Laboratory, Institute of Oceanology, Chinese Academy of Sciences), 1985. Bohai Sea Geology. Science Press, China, Beijing. 232 pp. (In Chinese).

Jacoby, J.G.C., D'Arrigo, R.D., 1989. Reconstructed northern hemisphere annual temperature since 1671 based on high latitude tree-ring data from North America. Climatic Change 14, 39–59.

Kjerfve, B., 1990. Manual for investigation of hydrological processes in mangrove ecosystems, Occasional Paper, RAS 79/002 and RAS/86/120. Unesco/United Nations Development Program Regional Mangrove Project. 79 pp.

Kukla, G., 1987. Loess stratigraphy in central China. Quaternary Science Reviews 6, 145–154.

Kullman, L., 2001. 20th century climate warming trend and tree-limit rise in the southern Scandes of Sweden. Ambio 30, 72–80.

Kusky, T., Guo, L., Xiang, S.B., Guo, X.Y., Xu, X.-Y., 2011. A critical examination of evidence for a Quaternary glaciation in Mt. Laoshan, Eastern China. Journal of Asian Earth Sciences 40, 403–416.

Lee, J.S., 1933. Quaternary glaciations in the Yangtze Valley. Bulletin of the Geological Society of China 13, 15–62.

Lee, J.S., 1934. Data relating to the study of the problem of glaciation in the Lower Yangtze Valley. Bulletin of the Geological Society of China 13, 395–433.

Lee, J.S., 1936. Confirmatory evidence of Pleistocene glaciation from the Huanshan, southern Anhui. Bulletin of the Geological Society of China 15, 279–284.

Leithold, E.L., 1989. Depositional processes on an ancient and modern muddy shelf, northern California. Sedimentology 36, 179–202.

Li, X., Du, N., 1999. The acid alkali free analysis of Quaternary pollen. Acta Botanica Sinica 41, 782–784 (In Chinese).

Li, F., Wang, H., Yan, Y.Z., Wang, Y., Zhang, J.Q., Zhao, C.R., Zhang, Y.F., Li, J.F., Lin, F., 2004. The significance of the depositional hiatuses on the coastal plain of west Bohai Bay since the late Quaternary period. Geological Survey and Research 27, 177–183 (In Chinese with English Abstract).

Li, P.Y., Xu, X.Y., Zhao, S., 2008. Coastal Loess and Glaciations. Ocean Press, Beijing. 337 pp. (In Chinese).

Lin, F., Wang, J.Z., Li, J.F., Pei, Y.D., Kang, H., 2005. Characteristics of microfossil assemblages and evolution of the sedimentary environment since the late Quaternary in the Laizhou Bay, Bohai Sea. Geological Bulletin of China 24, 879–884 (In Chinese with English Abstract).

Lisiecki, L.E., Raymo, M.E., 2005. A Pliocene–Pleistocene stack of 57 globally distributed benthic d18O records. Paleoceanography 20, PA1003.

Liu, T.S., 1985. Loess and the Environment. China Ocean Press, Beijing. 251 pp. (In Chinese).

Liu, T., 2009. Loess and Arid Environment. Anhui Science & Techonology Press, China, Hefei. 537 pp. (In Chinese).

Liu, T.S., Ding, Z.L., 1993. Stepwise coupling of monsoon circulations to global ice volume variations during the late Cenozoic. Global and Planetary Change 7, 119–130.

Liu, T., Ding, Z., 1998. Chinese loess and the paleomonsoon. Annual Review of Earth and Planetary Sciences 26, 111–145.

Liu, T.S., Ding, Z.L., Rutter, N.W., 1999. Comparison of Milankovitch periods between continental loess and deep sea records over the last 2.5 Ma. Quaternary Science Reviews 18, 1205–1212.

Liu, Z.F., Colin, C., Trentesaux, A., Siani, G., Frank, N., Blamart, D., Farid, S., 2005. Late Quaternary climatic control on erosion and weathering in the eastern Tibetan Plateau and the Mekong Basin. Quaternary Research 63, 316–328.

Liu, J., Saito, Y., Wang, H., Zhou, L.Y., Yang, Z.G., 2009. Stratigraphic development during the Late Pleistocene and Holocene offshore of the Yellow River delta, Bohai Sea. Journal of Asian Earth Sciences 36, 318–331.

Liu, Y., Lei, Y., Song, H., Bao, G., Sun, B., Wang, S., 2010. The annual mean lowest temperature renconstruction based on *Pinus bungeanas* (*Pinus bungeana* Zucc.) ring width in the Yulin Region, Shandong, China since AD 1616. Journal of Earth Environment 1, 28–35.

Lu, H.Y., Liu, X., Zhang, F.Q., An, Z.S., Dodson, J., 1999. Astronomical calibration of loess–paleosol deposits at Luochuan, central Chinese Loess Plateau. Palaeogeography, Palaeoclimatology, Palaeoecology 154, 237–246.

Lu, Y.C., Wang, X.L., Wintle, A.G., 2007. A new OSL chronology for dust accumulation in the last 130,000 yr for the Chinese Loess Plateau. Quaternary Research 67, 152–160.

Lü, H.B., Ren, X.H., Xu, M., Ou Yang, J.C., 2010. On the meltwater origin of potholes found on granite ridges — a consultation with Academician Shi Yafeng. Geological Review 56, 693–702 (In Chinese with English Abstract).

Marshall, S.J., Clark, P.U., 2002. Basal temperature evolution of North American ice sheets and implications for the 100-kyr cycle. Geophysical Research Letters 29, 2214.

Meng, Q., Han, M., Zhao, M., Jiang, A., 1999. A preliminary study of the Mihe River alluvial diluvial fan and the palaeochannels. Journal of Shandong Normal University (Natural Science) 14, 46–50 (In Chinese with English Abstract).

Nakagawa, T., Okuda, M., Yonenobu, H., Miyoshi, N., Fujiki, T., Gotanda, K., Tarasov, P.E., Morita, Y., Takemura, K., Horie, S., 2008. Regulation of the monsoon climate by two different orbital rhythms and forcing mechanisms. Geology 36, 491–494.

Nittrouer, C.A., Sternberg, R.W., 1981. The formation of sedimentary strata in an allochthonous shelf environment: the Washington continental shelf. Marine Geology 42, 201–232.

Paillard, D., 1998. The timing of Pleistocene glaciations from a simple multi-state climate model. Nature 391, 378–381.

Pederson, N., Cook, E.R., Jacoby, G.C., Peteet, D.M., Griffina, K.L., 2004. The influence of winter temperatures on the annual radial growth of six northern range margin tree species. Dendrochronologia 22, 7–29.

Pierrehumbert, R.T., 2000. Climate change and the tropical Pacific: the sleeping dragon wakes. PNAS 97, 1355–1358.

Porter, S.C., An, Z., 1995. Correlation between climate events in the North Atlantic and China during the last glaciation. Nature 375, 305–308.

Prescott, J.R., Hutton, J.T., 1994. Cosmic ray contributions to dose rates for luminescence and ESR dating: large depths and long-term time variations. Radiation Measurements 23, 497–500.

Rankl, J.G., 2004. Relations between total-sediment load and peak discharge for rainstorm runoff on five ephemeral streams in Wyoming. Water-Resources Investigations Report 02–4150. U.S. Geological Survey, Reston, Virginia, pp. 1–12.

Restrepo, J.D., Kjerfve, B., 2000. Water discharge and sediment load from the western slopes of the Colombian Andes with focus on Rio San Juan. Journal of Geology 108, 17–33.

Ruddiman, W.F., 2006. Orbital changes and climate. Quaternary Science Reviews 25, 3092–3112.

Ruddiman, W.F., Raymo, M.E., Martinson, D.G., Clement, B.M., Backman, J., 1989. Pleistocene evolution: northern hemisphere ice sheets and North Atlantic Ocean. Paleoceanography 4, 353–412.

SDSTC (The Committee of Science and Technology of Shandong Province), 1990. Investigation Reports of Coast & Beach Resources in Shandong Province. China Science and Technology Press, Beijing. 798 pp. (In Chinese).

Shao, X.M., Xu, Y., Yin, Z.Y., Liang, E.Y., Zhu, H., Wang, S., 2010. Climatic implications of a 3885-year tree-ring width chronology from the northeastern Qinghai–Tibetan Plateau. Quaternary Science Reviews 29, 2111–2122.

Shi, L., Zhai, Z., Wang, Q., Zhang, X., Yang, Z., 2009. Geochronological Study on Transgression Layers of the CQJ4 Borehole at Dagang area in Tianjin, China. Geological Review 55, 375–384.

Shi, Y.F., 2000. Glaciers and Related Environments in China. Science Press, Beijing. 410 pp. (In Chinese).

Shi, Y.F., 2010. On Prof. Lee's having misread debris flow deposits as Quaternary glaciations in the Lushan Area, Jiangxi Province. Geological Review 56, 683–692 (In Chinese with English Abstract).

Please cite this article as: Yi, L., et al., Late Quaternary linkage of sedimentary records to three astronomical rhythms and the Asian monsoon, inferred from a coastal boreho..., Palaeogeogr. Palaeoclimatol. Palaeoecol. (2012), doi:10.1016/j.palaeo.2012.02.020

Shi, Y.F., Deng, Y.X., 1982. The Quaternary flow deposits in the Lushan Area — evidence from the Yangjiaoling, northwest of Lushan. Chinese Science Bulletin 27, 1253–1258.
Shi, Y.F., Cui, Z.J., Li, J.J., 1987. Reassessment of Quaternary glaciation problems in Eastern China. Earth Sciences 2, 45–54 (In Chinese with English Abstract).
Smith, J.D., Foster, J., 1969. Geomagnetic reversal in Brunhes normal polarity epoch. Science 163, 565–567.
Stuiver, M., Reimer, P.J., 1993. Extended ^{14}C data base and revised CALIB 3.0 ^{14}C age calibration program. Radiocarbon 35, 215–230.
Sun, D.H., 2004. Monsoon and westerly circulation changes recorded in the late Cenozoic Aeolian sequences of Northern China. Global Planet Change 41, 63–80.
Sun, X.J., Luo, Y.L., Huang, F., Tian, J., Wang, P.X., 2003. Deep-sea pollen from the South China Sea: Pleistocene indicators of East Asian monsoon. Marine Geology 201, 97–118.
Sun, Y.B., Clemens, S.C., An, Z.S., Yu, Z.W., 2006. Astronomical timescale and palaeoclimatic implication of stacked 3.6-Myr monsoon records from the Chinese Loess Plateau. Quaternary Science Reviews 25, 33–48.
Sun, Y.B., Clemens, S.C., Morrill, C., Lin, X.P., Wang, X.L., An, Z.S., 2012. Influence of Atlantic meridional overturning circulation on the East Asian winter monsoon. Nature Geoscience 5, 46–49.
Tian, J., Wang, P.X., Cheng, X.R., Li, Q.Y., 2008. Astronomically tuned Plio-Pleistocene benthic d18O records from South China Sea and Atlantic–Pacific comparison. Earth and Planetary Science Letters 203, 1015–1029.
Treydte, K.S., Schleser, G.H., Helle, G., Frank, D.C., Winiger, M., Haug, G.H., Esper, J., 2006. The twentieth century was the wettest period in northern Pakistan over the past millennium. Nature 440, 1179–1182.
van Vugt, N., Steenbrink, J., Langereis, C.G., Hilgen, F.J., Meulenkamp, J.E., 1998. Magnetostratigraphy-based astronomical tuning of the early Pliocene lacustrine sediments of Ptolemais (NW Greece) and bed-to-bed correlation with the marine record. Earth and Planetary Science Letters 164, 535–551.
Vandenberghe, J., 1995. Timescales, climate and river development. Quaternary Science Reviews 14, 631–638.
Vandenberghe, J., 2003. Climate forcing of fluvial system development: an evolution of ideas. Quaternary Science Reviews 22, 2053–2060.
Villalba, R., 1994. Tree-ring and glacial evidence for the Medieval Warm Epoch and the Little Ice Age in southern South America. Climatic Change 26, 183–197.
Wang, P.X., 1999. Response of Western Pacific marginal seas to glacial cycles: paleoceanographic and sedimentological features. Marine Geology 156, 5–39.
Wang, B., 2006. The Asian Monsoon. Springer-Praxis Publishing, Chichester. 863 pp.
Wang, P.X., 2009. Global monsoon in a geological perspective. Chinese Science Bulletin 54, 1113–1136.
Wang, H., Fan, C., 2005. The ^{14}C database (II) on the circum-Bohai Sea-Coast. Quaternary Sciences 25, 141–156 (In Chinese with English Abstract).
Wang, Q., Tian, G.Q., 1999. The neotectonic settings of late Quaternary transgression on the eastern coastal plain of China. Journal of Geomechanics 5, 41–48 (In Chinese with English Abstract).
Wang, Q., Li, F., Li, Y., Gao, X., 1986. Shoreline changes in west-southern coastal plain of the Bohai Sea since 150 ka. In: Qin, Zhao (Eds.), Late Quaternary Sea-Level Changes. China Ocean Press, Beijing, pp. 62–71.
Wang, L., Sarnthein, M., Erlenkeuser, H., Grimalt, J., Grootes, P., Heilig, S., Ivanova, E., Kienast, M., Pelejero, C., Pflaumann, U., 1999. East Asian monsoon climate during the Late Pleistocene: high-resolution sediment records from the South China Sea. Marine Geology 156, 245–284.
Wang, Y., Cheng, H., Edwards, R.L., An, Z., Wu, J., Chen, C.-C., Dorale, J.A., 2001. A high-resolution absolute-dated Late Pleistocene monsoon record from Hulu Cave, China. Science 294, 2345–2348.
Wang, H., Li, F., Fan, C., Frechen, M., van Strydonck, M., Fei, D., Wang, Y., 2004. The ^{14}C database (I) on the circum-Bohai Sea-Coast. Quaternary Sciences 24, 601–613 (In Chinese with English Abstract).
Wang, Y., Cheng, H., Edwards, R.L., He, Y., Kong, X., An, Z., Wu, J., Kelly, M.J., Dykoski, C.A., Li, X., 2005. The Holocene Asian monsoon: links to solar changes and North Atlantic climate. Science 308, 854–857.
Wang, Y., Cheng, H., Edwards, R.L., Kong, X., Shao, X., Chen, S., Wu, J., Jiang, X., Wang, X., An, Z., 2008. Millennial- and orbital-scale changes in the East Asian monsoon over the past 224,000 years. Nature 451, 1090–1093.
Webster, P.J., Magana, V.O., Palmer, T.N., Shukla, J., Tomas, R.A., Yanai, M., Yasunari, T., 1998. Monsoons: processes, predictability, and the prospects for prediction. Journal of Geophysical Research 103, 14451–14510.
Wehausen, R., Brumsack, H.-J., 2002. Astronomical forcing of the East Asian monsoon mirrored by the composition of Pliocene South China Sea sediments. Earth and Planetary Science Letters 201, 621–636.
Weltje, G.J., 1997. End-member modeling of compositional data: numerical–statistical algorithms for solving the explicit mixing problem. Mathematical Geology 29, 503–549.
Wheatcroft, R.A., Wiberg, P.L., Alexander, C.R., Bentley, S.J., Drake, D.E., Harris, C.K., Ogston, A.S., 2007. Post-depositional alternation and preservation of sedimentary strata. In: Nittrouer, C.A., et al. (Ed.), Continental Margin Sedimentation: from Sediment Transport to Sequence Stratigraphy. BlackWell Publishing, pp. 101–155.
White, E.M., 2002. Comment on "Late Holocene lake sedimentology and climate change in Southern Alberta, Canada" by Campbell. Quaternary Research 58, 397-397.
Wu, S., Yu, Z., Zou, D., Zhang, H., 2006. Structural features and Cenozoic evolution of the Tan-Lu Fault Zone in the Laizhou Bay, Bohai Sea. Marine Geology & Quaternary Geology 26, 101–110 (In Chinese with English Abstract).
Xiao, J., Chang, Z., Si, B., Qin, X., Itoh, S., Lomtatidze, Z., 2009. Partitioning of the grain-size components of Dali Lake core sediments: evidence for lake-level changes during the Holocene. Journal of Paleolimnology 42, 249–260.
Xue, C., Ding, D., 2008. Weihe River–Mihe River Delta in South Coast of Bohai Sea, China: sedimentary sequence and architecture. Scientia Geographica Sinica 28, 672–676 (In Chinese with English Abstract).
Yan, Y.Z., Wang, H., Li, F., Li, J.F., Zhao, C.R., Lin, F., 2006. Sedimentary environment and sea-level fluctuation revealed by Borehole BQ1 on the west coast of the Bohai Bay, China. Geological Bulletin of China 25, 357–382 (In Chinese with English Abstract).
Yancheva, G., Nowaczyk, N.R., Mingram, J., Dulski, P., Schettler, G., Negendank, J.F.W., Liu, J., Sigman, D.M., Peterson, L.C., Haug, G.H., 2007. Influence of the intertropical convergence zone on the East Asian monsoon. Nature 445, 74–77.
Yang, Z.G., Lin, H.M., 1991. Quaternary Processes in Eastern China and Their International Correlation. Geological Publishing House, Beijing. 137 pp.
Yao, J., Yu, H.J., Xu, X.Y., Yi, L., Su, Q., 2010. Deposition characteristics in brine aquifers and brine formation in Laizhou Bay Area. Advances in Marine Science 28, 473–477 (In Chinese with English Abstract).
Yi, L., 2010. Environment history of south Bohai Sea during the past 250 ka: Inferred from the Lz908 borehold. Ph.D. Dissertation, Yantai Institute of Coastal Zone Research, Chinese Academy of Sciences. (In Chinese).
Yim, W.W.-S., Ivanovich, M., Yu, K.-F., 1990. Young age bias of radiocarbon dates in pre-Holocene marine deposits of Hong Kong and implications for Pleistocene stratigraphy. Geo-Marine Letters 10, 165–172.
Yu, H.J., Han, D.L., Liu, X., Shan, Q.M., 1999. Study on the disintegration of marine stratum in the northern shelf region of nearshore seas of China. Acta Oceanologica Sinica 21, 83–89 (In Chinese with English Abstract).
Yu, Z., Wu, S., Zou, D., Feng, D., Zhao, H., 2008. Seismic profiles across the middle Tan-Lu fault zone in Laizhou Bay, Bohai Sea, eastern China. Journal of Asian Earth Sciences 33, 383–394.
Zhang, Y.X., Xue, Y.Q., Chen, H.H., 1996. Characteristics and its environments of seawater deposited in Late Pleistocene layers in the south Laizhou Bay. Acta Oceanologica Sinica 18, 61–68.
Zhang, Y., Dong, S., Shi, W., 2003. Cretaceous deformation history of the middle Tan-Lu fault zone in Shandong Province, eastern China. Tectonophysics 363, 243–258.
Zhang, S.R., Lu, X.X., Higgitt, D.L., Chen, C.-T.A., 2007. Recent changes of water discharge and sediment load in the Zhujiang (Pearl River) Basin, China. Global and Planetary Change 60, 365–380.
Zhang, P., Cheng, H., Edwards, R.L., Chen, F., Wang, Y., Yang, X., Liu, J., Tan, M., Wang, X., Liu, J., An, C., Dai, Z., Zhou, J., Zhang, D., Jia, J., Jin, L., Johnson, K.R., 2008a. A test of climate, sun, and culture relationships from an 1810-year Chinese cave record. Science 320, 940–942.
Zhang, Z.L., Liu, E.F., Zhang, Y., Xin, L.J., 2008b. Environmental evolution in the salt-water intrusion area south of Laizhou Bay since late Pleistocene. Journal of Geographical Sciences 18, 37–56.
Zhao, S., 1986. Transgression and coastal changes in Bohai Sea and its vicinities since the Late Pleistocene. In: Qin, Zhao (Eds.), Late Quaternary Sea-Level Changes. China Ocean Press, Beijing, pp. 53–62.
Zhao, S., 1991. China Shelf Sea desertization and its derived deposits during the last stage of late Pleistocene. Oceanologia and Liminologia Sinica 22, 285–293 (In Chinese).
Zhao, S., 1995. Shelf Desertification. Ocean Press, China, Beijing. 194 pp. (In Chinese).
Zhao, S., 2010. Low-altitude Glaciations in the Eastern China. Ocean Press, Beijing. 392 pp. (In Chinese).
Zhao, S., Yang, G., Cang, S., Zhang, H., Huang, Q., Xia, D., Wang, Y., Liu, F., Liu, C., 1978. On the marine stratigraphy and coastlines of the western coast of the gulf of Bohai. Oceanologia and Liminologia Sinica 9, 15–25 (In Chinese with English Abstract).
Zhou, S.Z., 2006. Are all potholes markers of Quaternary glaciations? Quaternary Sciences 26, 117–125 (In Chinese with English Abstract).
Zhuang, Z.Y., Xu, W.D., Liu, D.S., Zhuang, L.H., Liu, B.Z., Cao, Y.Y., Wang, Q., 1999. Division and environmental evolution of late Quaternary marine beds of S3 hole in the Bohai Sea. Marine Geology & Quaternary Geology 19, 27–35 (In Chinese with English Abstract).